JOURNAL OF GEOPHYSICAL RESEARCH, VOL. 98, NO. B2, PAGES 2039–2060, FEBRUARY 10, 1993

Thermal Constraints on the Zone of Major Thrust Earthquake Failure: The Cascadia Subduction Zone

R. D. HYNDMAN AND K. WANG

Pacific Geoscience Centre, Geological Survey of Canada, Sidney, British Columbia

Constraints on the seismogenic portion of the subduction thrust zone along the Cascadia margin are provided by the thermal regime. The zone of stick-slip "locked" behavior where earthquakes can nucleate may be limited downdip by a temperature of about 350 °C, and the transition stable sliding zone into which coseismic displacement can extend by a temperature of approximately 450 °C. The seaward limit of the stick-slip zone may be associated with the dehydration of stable sliding clays at 100 to 150 °C and dissipation of high pore pressures in the area of the deformation front. Temperatures on the thrust have been estimated by numerically modelling the thermal regimes along three profiles crossing the margin with constraints provided by surface heat flow and detailed structural information, particularly at southern Vancouver Island. The models that best fit the heat flow data have negligible shear strain heating. The Cascadia subduction margin is unusually hot as a consequence of the very young plate age and the thick insulating sediment section on the incoming plate; the temperature at the top of the oceanic crust at the deformation front is about 250 °C. As a result, the modelled zone of stick-slip seismogenic behaviour is restricted to a narrow zone beneath the continental slope and outer shelf, with the transition zone extending to the inner shelf. The seismogenic zone is wider off the Olympic Peninsula compared to off southern Vancouver Island because of the much shallower thrust dip angle and the slightly older incoming plate. The profile off Oregon is found to have intermediate width zones. An important assumption, well justified only off southern Vancouver Island, is that the thrust detachment is located at the top of the downgoing oceanic crust. The same modelling technique shows that more typical subduction zones with older incoming oceanic lithosphere such as central Chile have thermally restricted seismogenic zones that are much wider, commonly extending well beneath the coast. Support for the position of the Cascadia locked zone from the thermal results is provided by a comparison of the horizontal and vertical interseismic deformation predicted by simple dislocation models with the observed rates from tide gauge and geodetic surveys on adjacent coastal regions. The general agreement indicates that any seismic "locked zone" must be located offshore where the subduction thrust fault is less than about 20 km deep and where the contact is between the oceanic crust and the accreted sedimentary wedge, not between the oceanic and continental crusts. The restriction to an offshore zone provides an important limit to the maximum magnitude and to the ground motion and seismic hazard from subduction megathrust earthquakes in southwestern British Columbia, Washington, and Oregon.

INTRODUCTION

The largest earthquakes in the world occur on the primary thrust or detachment surface of subduction zones and most convergent margins have experienced such megathrust events in historical times. The Cascadia margin (Figure 1) is unusual in that there have been no megathrust earthquakes during the 150 to 200 year historical period [see *Rogers*, 1988; *Heaton*, 1990]. Three possibilities exist: (1) that there is no present convergence, (2) that the convergence is being taken up by aseismic slip, and (3) that large earthquakes do occur but that the last event was prior to the historical period. The first two options imply that the seismic risk estimates for the region based on historical seismicity are appropriate. The third option implies that there is a potential for very large and damaging earthquakes that is not included in most past risk estimates.

Convergence across the Cascadia margin over the past few million years is indicated by plate tectonic analyses of magnetic anomalies and transform fault orientations [e.g., *Riddihough*, 1984; *DeMets et al.*, 1987] and by a wide variety of data along the deformation front [e.g., *Riddihough and Hyndman*, 1976; *Carson*, 1977; *Cochrane et al.*, 1988; *Davis and Hyndman*, 1989; *Hyndman et al.*, 1990]. Contemporary plate convergence is implied by seismic moment release data and by geodetic data. The average motions estimated from the rate of seismic moment release around the transform fault boundaries of the Juan de Fuca plate system from the past 70 years of seismic data are very close to the longer term average rates from magnetic anomaly analysis [*Hyndman and Weichert*, 1983]. Convergence across the margin at a rate of about 50 mm yr^{-1} is required. Evidence for present shortening across the margin also comes from geodetic measurements on land near the coast [e.g., *Savage et al.*, 1991].

Heaton and Kanamori [1984], *Heaton and Hartzell* [1987], and *Rogers* [1988] have compared the Cascadia subduction zone to other convergent margins around the world. All but one of the 6 margins where young oceanic crust is being subducted studied by *Rogers* [1988] have had very large (i.e., magnitude 8 or greater) historical events. Rogers noted that, like the Cascadia margin, most of the other areas have had little or no seismicity on the main thrust plane between the times of the large events.

Evidence that major earthquakes do occur on the Cascadia margin approximately every 300 to 600 years comes from extensive paleoseismic data, from the margins of southern British Columbia, Washington and Oregon, including indications of abrupt vertical motion and shaking in coastal regions and of periodic turbidite flows simultaneously in a number of deep-sea channels (examples of the extensive recent literature are *Atwater* [1987], Atwater et al. [1991]; *Darienzo and Peterson* [1990]; and

Paper number 92JB002279.
0148-0227/93/92JB-002279$05.00

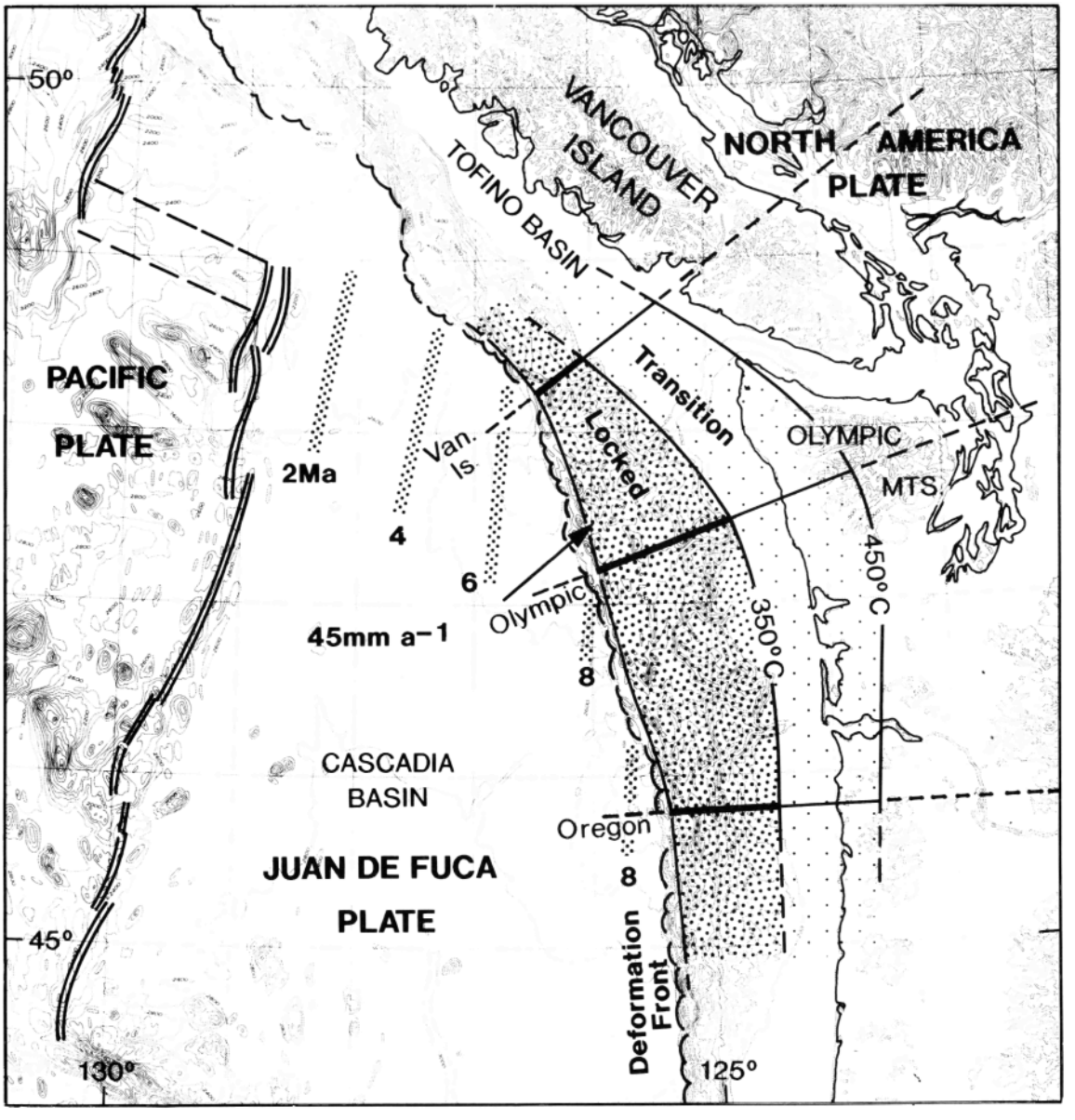

Fig. 1. Cascadia margin area showing the locations of the three model profiles with the computed limits of stick-slip "locked" and stable sliding "transition" zones for the subduction thrust plane. The recognized uncertainties give error limits of about ±30 km in the landward boundaries of the locked and transition zones.

Adams, [1990]). These data support the third option above, that large earthquakes do occur.

If it is accepted that this margin is subject to large thrust events, the next important questions for risk analysis include, what is the maximum magnitude and where on the thrust plane can they occur. The mechanisms which restrict the seismogenic zone on subduction zone thrusts have been discussed by a number of authors; the possible limits at the landward end include temperature, the composition and state of the contact material, and the slab dip angle [e.g., *Tichelaar and Ruff*, 1991]. *Ruff and Kanamori* [1983] have suggested that the maximum depth of the "brittle" zone is determined by the depth to the basalt-eclogite transition, expected to be below a depth of 30-35 km. At the seaward end, *Byrne et al.* [1988] have suggested that the limit is where the subduction thrust cuts unconsolidated or semi-consolidated sediments.

In this article we examine thermal constraints to the Cascadia "locked zone" on which very large thrust earthquakes may occur, developing in more detail the initial estimates presented by *Hyndman et al.* [1989] and *Davis et al.* [1990]. Estimates of the thermal constraints on the locked zone have also been presented by *Blackwell* [1991]. The landward limit is taken to be where the temperature exceeds that for the stick-slip behaviour that allows seismic instability. The seaward limit of the seismogenic zone may be where the thrust detachment faults cut relatively unconsolidated sediments containing stable sliding clays, perhaps with high pore pressures. We emphasize that while temperature may provide limits to where earthquakes can occur, there may be other reasons why earthquakes are not generated within the thermally allowable range. Most previous analyses of this problem have been for generic subduction zones with average characteristics, ignoring the large variability. Here we attempt

detailed modelling of specific sections. We concentrate on the northern Cascadia margin along the west coast of Vancouver Island where there is particularly complete structure and thermal data, but models have been generated for the Olympic margin of northern Washington and for the margin of Oregon. Some analysis of the sensitivity of the modelled thermal regime to variations in subduction parameters has also been undertaken.

A check on the estimated extent of the seismogenic zones can be provided by a comparison of the predicted interseismic horizontal and vertical deformation with the contemporary rates observed. This comparison was made by *Savage et al.* [1991] for the central Cascadia, Olympic margin using temperature estimates from *Davis et al.* [1990]. We provide a more detailed comparison for the three Cascadia profiles.

The downdip extent of the seismogenic zone should provide information on the maximum magnitude of events. Variations in thermal regimes may also explain why some subduction zones are subject to very large thrust earthquakes that break a long distance downdip on the main thrust, while other areas have only smaller events that fail a short distance downdip. An important related question is why in some subduction zones most of the relative plate motion occurs in large earthquakes, while in others only a small fraction appears to occur in this way, with much of the motion being aseismic [e.g., *Kanamori,* 1977].

In the sections below we first discuss the geometry of the main detachment thrust, second, develop thermal models that constrain the portions of this thrust that exhibit different fault behaviours, (e.g., the zone of stick-slip seismogenic behaviour), and finally, compare the interseismic deformation predicted by the thermally constrained stick-slip and transition zones with contemporary deformation data.

GEOMETRY OF THE MAIN DETACHMENT THRUST

In this section we provide a description of the detachment on which the ocean-continent underthrusting occurs beneath the southern Vancouver Island margin where the structure is particularly well constrained. First, it is shown that the main detachment is near the base of the sediment section, close to or at the top of the downgoing oceanic crust. Second, the location of the top of the downgoing oceanic crust is constrained by a variety of geophysical data from seaward of the deformation front to beneath the coastal region. In this article we do not deal with faults that cut upward to the surface from the main detachment at positions landward of the deformation front. Although they may be seismogenic, they accommodate only a small amount of shortening compared to the main subduction thrust detachment.

The deformation and detachment of the incoming sediments on the Juan de Fuca plate has been well delineated by multichannel seismic lines across the Vancouver Island margin [*Davis and Hyndman,* 1989; *Hyndman et al.*, 1990; *Spence et al.*, 1991a; 1991b]. The sediments beneath the offshore Cascadia basin that are being incorporated into the accretionary sedimentary prism are about 3 km thick, consisting of 1.5 km of hemipelagic sediments beneath 1.5 km of Pleistocene turbidites. Portions of the section were sampled by Deep Sea Drilling Project Leg 18 to the north and south of the study area [*Kulm et al.*, 1973]. The sediment is scraped off the incoming oceanic crust at the deformation front forming a series of anticlinal ridges parallel to the margin, generally over seismically imaged thrust faults. Much of the convergence shortening occurs over a narrow zone, although it appears to continue at a decreasing rate across the accretionary wedge [e.g., *Adams,* 1984].

An important conclusion from the seismic data is that the thrust faults penetrate close to the top of the underlying oceanic crust in this area, so almost all of the incoming sediment is scraped off [*Davis and Hyndman,* 1989; *Hyndman et al.*, 1990] (Figure 2). It is possible that further landward the detachment steps up into the overlying accretionary wedge, but several shallowly dipping thrusts extending from beneath asymmetric ridges on the continental slope to near the downgoing oceanic crust beneath the continental shelf [see *Hyndman et al.*, 1990] make this unlikely. Mass balance calculations also show that the volume of sediment in the accretionary wedge can account for all of the incoming sediment during the current phase of subduction commencing in the Eocene. The main detachment being located at the base of the sediment section is in contrast to many other margins with large accretionary wedges, where the detachment occurs within the sediment section [e.g., *von Huene and Scholl,* 1991]. Off Oregon, recently acquired seismic data shows the detachment near the top of the oceanic crust in some sections and about 0.5 km higher within the sediment column in others [*MacKay et al.*, 1992]. The latter detachments may step down to near the crust further inland; an example of such a downward step in the detachment is seen in a seismic section across the Nankai margin of southern Japan [*Moore et al.*, 1990]. A detachment higher in the section will first significantly affect the location of the seaward end of the seismogenic zone, since the temperature for clay dehydration on the thrust surface may not occur to a more landward position. The effect on the landward end of the seismogenic zone may also be significant because the initial temperature on the thrust plane at the deformation front will be lower, and thus the temperatures lower to a considerable distance downdip along the thrust. Our modelling assumes that the detachment is near the top of the oceanic crust which we believe is valid for the Vancouver Island margin, but we note that accurate thrust plane temperatures for other areas require knowledge of the detachment level in the accretionary wedges.

The top of the oceanic crust across the Vancouver Island margin is a smooth gently dipping surface defined by discontinuous but clear seismic reflections from beneath the

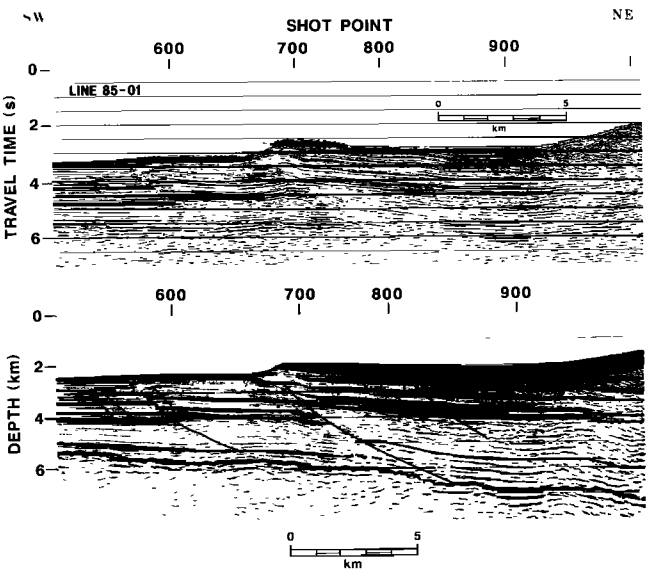

Fig. 2. Multichannel seismic reflection time and depth sections of the deformation front area off southern Vancouver Island, showing the thrusts extending to near the top of the oceanic crust.

Cascadia abyssal plain to a depth of about 45 km beneath southern Vancouver Island [*Hyndman et al.*, 1990; *Spence et al.*, 1991b] (Figures 2 and 3). As noted by *Davis and Karsten* [1986] the present Juan de Fuca plate surface is particularly smooth with very few seamounts; the seismic reflection data indicate that the subducted portion is also smooth. *Calvert and Clowes* [1991] have argued that the strong reflector in places marking the top of the crust requires high pore pressure. The location of the top of the oceanic crust is also defined by seismic refraction data [e.g., *Spence et al.*, 1985; *Drew and Clowes*, 1990], dipping inland to about 30 km depth near the coast. These depths are in good agreement with the reflection depths obtained by converting the travel times to reflector "F" (Figure 3) to depth using the refraction velocities [see detailed studies in *Green*, 1990].

The third constraint on the position of the oceanic crust comes from Benioff-Wadati seismicity [e.g., *Rogers et al.*, 1985; 1990; *Crosson and Owens*, 1987]. The young age of the Juan de Fuca plate restricts the low temperatures where Benioff-Wadati earthquakes can occur to a thin zone probably in the uppermost mantle (earthquakes can occur to about 800°C in mantle rocks compared to about 350°C for crustal rocks). Using the same velocity structure in the earthquake location routine as used to convert the reflection times to depth, most of the well located Benioff-Wadati events beneath the Vancouver Island margin are just below the top of the oceanic crust as defined by the reflection and refraction data (see below). The uncertainties are such that they may be in the uppermost mantle as suggested by the thermal data. In this area, the dip of the oceanic crust increases from 3 to 4° seaward of the deformation front, to 10° under the edge of the shelf and to 15° beneath the coast (Figure 3). In the models we have neglected probable steepening of the plate dip beyond where its depth is about 60 km. The accretionary wedge backstop is probably formed by the landward dipping volcanic Crescent terrane that approaches the seafloor beneath the inner shelf [*Hyndman et al.*, 1990].

Along a transect through the Olympic Mountains of northern Washington, the dip at the deformation front is similar, 3 to 4°. However, the accretionary wedge is nearly 4 times as wide, extending well inland of the coast to form the core of the Olympic Mountains [*Tabor and Cady*, 1978], and the landward steepening of the dip is much more gradual [e.g., *Taber and Lewis*, 1986; *Crosson and Owens*, 1987] (see dashed line in Figure 6a). The dip at the coast is about 8 to 9°, and 15° is reached only 150 km further inland. The shallow dip may result from upward warping of the subducting plate in this corner of the coastline [e.g., *Rogers*, 1983] and the wide accretionary wedge may be the result of sediment transport northward along the margin from off Washington and Oregon into this corner as a consequence of the oblique subduction. The seaward portion of the accretionary wedge structure [e.g., *Snavely*, 1987; *Snavely and Wagner*, 1981; *Silver*, 1972] is very similar to that inferred for off southern Vancouver Island.

Off northern Oregon the structure and plate dip beneath the coastal region are not well constrained by the seismicity [e.g., *Crosson and Owens*, 1987] but they appear to be similar to those off Vancouver Island. The sediment structure and plate dip beneath the outer shelf is also similar based on multichannel seismic reflection data [*MacKay et al.*, 1992].

CONSTRAINTS ON THE SEISMOGENIC PORTION OF THE THRUST PLANE

Downdip Divisions of the Thrust Fault

The deformation behaviour of rocks under deviatoric stress changes from brittle at low temperatures and pressures to plastic at high temperatures and pressures. Such a "brittle-ductile" transition has in the past usually been considered the reason fault earthquakes are largely confined to the upper 10 to 20 km depth of the crust. Recent analyses of fault mechanics have shown however, that earthquakes are a manifestation of frictional instability on the fault zone, not of bulk rock rheology, and that the transition to a fully plastic behaviour only gives a maximum earthquake fault propagation depth. Earthquake initiation may be limited to lower temperatures. Within the brittle or semi-brittle region, the fault motion may be by stable sliding under some conditions or by unstable stick-slip under other conditions. Earthquakes can initiate only in the latter case. The seismogenic zone of the main subduction thrust fault is thus constrained by changes in fault zone behaviour with downdip distance. A synoptic model for continental shear zones has been suggested by *Scholtz* [1988]. In this section, we apply the results of frictional stability analysis to the thrust zone and propose that the thrust

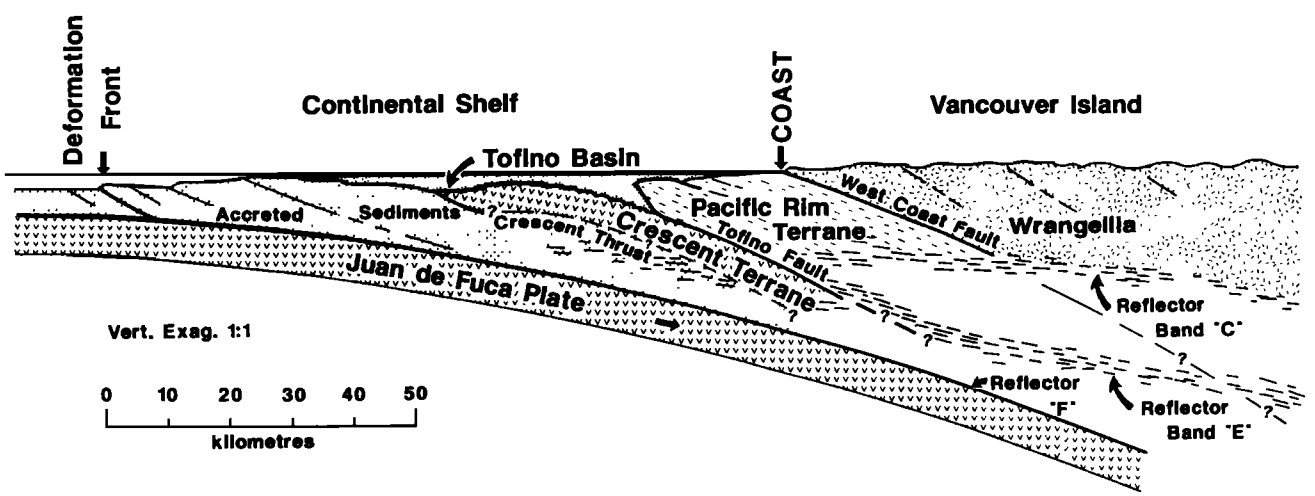

Fig. 3. Structural cross-section across the margin through southern Vancouver Island [after *Hyndman et al.*, 1990], showing the position of the top of the oceanic crust that is taken to be the main subduction thrust.

consists of four segments downdip from the deformation front, following the model of *Scholtz* [1988].

Four distinct zones of the subduction thrust may be defined (Table 1). (1) A zone of stable sliding at the seaward end of the thrust detachment, for example in unconsolidated or clay rich sediments. (2) The "locked" zone with stick-slip or unstable sliding behaviour which allows elastic strain to be stored between abrupt motion events. Earthquakes may nucleate in this zone. (3) A transition zone, with stable sliding behaviour. In this latter zone, the slip deficit will move partly in large earthquake displacement with decreasing displacement away from the stick-slip zone, and partly in post-seismic slip [e.g., *Stuart*, 1988]. (4) The zone of plastic behaviour associated with high temperatures that extends to great depths. Motion on this latter portion of the detachment should be nearly continuous throughout the cycle of coseismic and interseismic periods. How this division bears on earthquake generation can be best understood through analysis of the fault zone stability.

Based on rock and metal friction experiments, *Dieterich* [1981] and *Ruina* [1983] derived an empirical constitutive relation for friction in terms of sliding velocity V and a series of state variables. A critical characteristic of the frictional behaviour as depicted by this constitutive relation and as observed in the laboratory, is the strong velocity dependence of the shear resistance $\tau = \sigma_n \mu$, where σ_n is the normal stress and μ is the frictional coefficient. In laboratory experiments, when sliding changes from one steady state to another, e.g., due to a change in equipment controlled sliding velocity V, τ evolves to a new steady state value through a transient response. By the constitutive relation [*Dieterich*, 1981; *Ruina*, 1983], the steady state value of τ is:

$$\tau^{ss} = \sigma_n \mu^{ss} = \sigma_n [\mu_o + (a-b) \ln(\frac{V}{V^*})] \quad (1)$$

where the physical quantity $a - b$ is determined by the rheology of the material at the friction surface and environmental effects involving water and chemical reactions and V^* is an arbitrarily defined reference velocity. The overall behaviour of friction can be considered as this steady state response convolved with the transient response.

TABLE 1. Thrust Fault Zone Downdip Divisions

Zone	Interseismic	Coseismic	Mechanism
Seaward zone	Little motion	No seismic initiation, displacement of most of the slip deficit	Stable sliding
Seismogenic "locked" zone	No motion, allows elastic strain to accumulate	Earthquake initiation, displacement of the total slip deficit	Stick-slip, unstable
Transition zone	Rate increases downdip from zero to plate rate	Displacement on seaward portion, decreasing downdip	Stable sliding
"Creep" zone	Steady motion at plate rate	No motion	Plastic deformation

From equation (1),

$$a - b = \frac{\partial \mu^{ss}}{\partial (\ln V)} = \frac{V}{\sigma} \frac{\partial \tau^{ss}}{\partial V} \quad (2)$$

If, to the first order, $a - b$ is taken to be zero, (1) reduces to Amonton's law of friction, of which Byerlee's friction law [*Byerlee*, 1978] at low loads (< 200 MPa) is a special case for rocks. However, for the stability of faults under dynamic loading, the second order effect ($a - b \neq 0$) must be considered. As shown by *Tse and Rice* [1986], the sign of $a - b$ determines the stability of a fault. If $a - b > 0$, any positive perturbation in sliding velocity results in an increase in the steady state shear resistance τ^{ss} and the sliding is stable. This case is referred to as velocity strengthening. Conversely, for the case in which $a - b < 0$, there is velocity weakening and the sliding will be unstable, unless the normal stress is larger than a certain critical value such that only a large sudden increase of velocity can cause unstable sliding, a situation known as conditional stability [*Rice and Ruina*, 1983; *Gu et al.*, 1984]. Unstable frictional motion ($a - b < 0$) of faults in the earth appears as stick-slip. During the "stick" or locked phase, the shear stress is sustained at the locked segment of the fault zone; during the very short "slip" phase, large stress drop occurs. Fault segments with $a - b > 0$ in contrast will not initiate earthquakes.

Landward Limit of the Seismogenic Zone

There appears to be a critical temperature for the transition between unstable and stable sliding behaviour. While it undoubtedly depends on the composition of the material at the fault interface, both laboratory data for some crustal rocks and field estimates for crustal earthquakes give temperatures of 300 to 350°C. *Tse and Rice* [1986], using data for dry granite from *Stesky* [1975], found that parameter $a - b$ is positively correlated to temperature for granite samples, and the transition from velocity weakening to velocity strengthening occurs in the temperature range of 300 to 350°C (Figure 4a). This temperature range corresponds approximately to the onset of quartz plasticity and is believed to be the transition from brittle to semi-brittle behaviour of continental crustal rocks [*Scholtz*, 1990]. *Blanpied et al.* [1991] have extended the laboratory data to include the effect of pore fluids, and found a similar maximum temperature for velocity weakening in the range of 325-350°C. A maximum depth of earthquakes in most continental areas has been found to be at a temperature of 300 to 350°C [*Brace and Byerlee*, 1966; *Chen and Molnar*, 1983; *Tse and Rice*, 1986; *Wong and Chapman*, 1990]. This also corresponds approximately to the temperature at the maximum depth of earthquakes within the Vancouver Island continental crust above the subducting plate (see below), and is within the common range of estimated temperatures for the downdip limit of seismic coupling at many subduction zones [*Tichelaar and Ruff*, 1992].

To determine the depth limit of the stick-slip segment of a convergent margin thrust fault, we need to know the temperature of the velocity weakening - velocity strengthening transition for the material and conditions on the fault. A convergent margin thrust fault may separate dissimilar rock types, but the behaviour of the fault should depend on the "softer" overlying forearc material, i.e., accreted sediments in the case of Cascadia. This is indicated by the study of fossil subduction thrust zones [*Scholtz*, 1990, p.291]. There is no experimental data specifically for such consolidated sediments, and we have taken 350°C from the discussion above as the reference temperature for the sign change

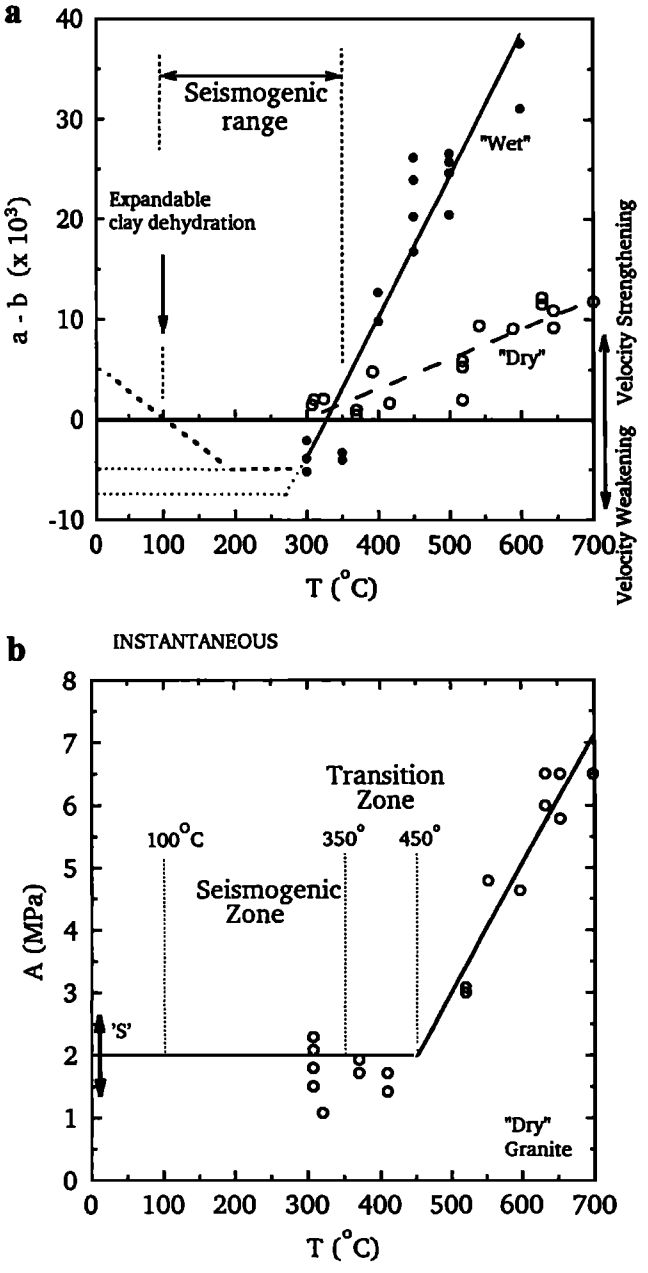

Fig. 4. (a) The velocity strengthening-velocity weakening behaviour at 325-350°C following *Tse and Rice* [1986] using "dry" granite data from *Stesky* [1975] and "wet" data from *Blanpied et al.* [1991]. The dehydration of stable sliding clays at 100-150 °C provides a low temperature limit to the seismogenic range. (b) The instantaneous shear stress [*Tse and Rice*, 1986] showing the rapid increase above 400-450 °C. 'S' is range of room temperature data from *Dietrich* [1981].

of a - b at Cascadia thrust zone, defining the depth limit of the stick-slip segment of the subduction thrust; there is an uncertainty of at least ± 25°C.

Earthquakes, including foreshocks and aftershocks, should not nucleate at depths where the temperature exceeds 350°C along the trust fault. The downdip limit of the stable sliding segment is taken to be at a temperature of about 450°C, the onset of feldspar plasticity [*Scholtz*, 1990], above which ductile behaviour will dominate for continental, and forearc rocks. The downdip limit of the transition zone is less well constrained than the limit of the locked zone, for example the former has an important strain rate dependence. A temperature of about 450°C also marks the beginning of a rapid increase of "instantaneous" frictional stress [*Tse and Rice*, 1986] (Figure 4b) and thus where it becomes difficult to propagate abrupt earthquake failure. During the interseismic period between major events, the deep stable sliding segment provides the transition from the totally locked portion to the free moving portion, and therefore it is referred to as the transition zone.

The coseismic and short term post-seismic behaviour of the transition zone is complex. At the seaward end of the transition zone, most of the slip deficit moves in the seismic event, while at the landward end most of the motion is probably in short term (days to months) post-seismic sliding [e.g., *Stuart*, 1988]. It should be noted that although earthquakes cannot nucleate in the transition zone, coseismic rupture will extend some distance into it.

In summary, the stick-slip seismogenic zone is predicted to extend downward to about 350°C and the transitional stable sliding zone to about 450°C. We emphasize that the seismogenic zone based on temperature only restricts earthquake nucleation to be outside this portion of the thrust, but does not indicate that earthquakes must occur within it. There are many other environmental factors that control the sign of a - b, such as the existence of high pore fluid pressures. Earthquake displacement is expected to extend downdip to between these two temperature limits, with decreasing offset beyond where 350°C is reached.

Seaward Limit of Seismogenic Zone

Stable sliding behaviour is expected to occur in the relatively unconsolidated sediments in the region of the subduction zone deformation front. *Byrne et al.* [1988] observed globally that earthquakes usually do not extend up-dip to the trench axis. The upper boundary between seismic and aseismic behaviour, which appears to be defined by both smaller earthquakes between large events, and by the aftershocks of large events was described as the "seismic front". They suggested that aseismic slip occurs on the seaward part of the thrust plane because of the stable slip properties of unconsolidated and semi-consolidated sediments. The seismic behaviour could then be limited to locations where the overlying material is crystalline continental or arc crust, or very consolidated sediments.

For margins with large accretionary wedges, sediments may occur in the upper hanging wall to great depths (see Figure 3 for Vancouver Island margin), and any seismogenic thrusting downdip to depths of several tens of kilometres must occur with consolidated sediments on at least one side of the thrust plane. Older accreted sediments loaded by a thick overlying section are progressively dewatered and consolidated and altered by chemical diagenesis. They thus probably will exhibit stick-slip behaviour. In fact, the association of "excess trench sediments" with great subduction zone earthquakes [*Ruff*, 1989] has the suggested mechanism that coherent sediments at elevated temperatures and pressures form a particularly homogeneous and strong contact zone between the plates. In contrast, in subduction zones with little sediment, the thrust will usually separate igneous rocks and small scale roughness will give small scale asperities and small maximum size earthquakes.

An important control of slip behaviour in sediments may be the presence or absence of substantial clay; clays usually represent a significant proportion of the incoming sediments that are accreted to the margin. *Wang* [1980] has summarized the laboratory data for the mechanical properties of clayey sediments [see also *Chamley*, 1989]. *Wang and Mao* [1979] found that the shear

stress required to initiate sliding is very much lower for clays compared to rock-on-rock sliding [see also *Logan and Rauenzahn*, 1987]. The starting friction coefficients for montmorillonite (one member of the smectite family), chlorite and illite were found to be 0.08, 0.12 and 0.22 respectively compared to 0.6-0.8 for rock-rock sliding. Sliding was stable up to at least 300 MPa effective normal stress for all of the clays studied. They postulated that expandable clays such as montmorillonite may remain stable even after most free water (not bound water) is lost due to loading fluid expulsion, but nonexpandable clays such as kaolinite, illite and chlorite may exhibit stick-slip behaviour after most free water is lost. While kaolinite and chlorite dehydrate at relatively high temperatures (about 300 and 600°C respectively), most smectite will have transformed by 100 to 150°C [e.g., *Chamley*, 1989, Figure 5a; *Jennings and Thompson*, 1986; *Hower et al.*, 1976, Figure 5b]. *Vrolijk* [1990] has pointed out that decollements in subduction zones tend to occur in smectite-rich horizons, and that the depth to the most seaward decollement earthquakes often approximately coincides with the point where the estimated temperature reaches the smectite-illite transition.

From the thermal models described below, the Cascadia margin is exceptionally hot, and smectite clays should have been dehydrated in the sediments well above the top of the oceanic crust seaward of the deformation front where the estimated temperature is about 250°C. Thus, if the dehydration of expandable clay between 100 and 150°C is the controlling factor, the seaward limit of stick-slip behaviour will be where the active frontal thrusts reach a depth of 1 to 2 km, just seaward of where they reach the depth of the main detachment near the oceanic crust, i.e., about 5 km landward of the deformation front. In contrast, most subduction zone accretionary prisms have much lower temperatures. Thus, they may have stable sliding clays throughout their sections, explaining the results of *Byrne et al.* [1988].

The other mechanism that may limit stick-slip behaviour near the seaward end of the subduction thrust is high pore pressures. High pore pressures beneath the lower slope were inferred by *Davis and Hyndman* [1989] based on critical taper theory. They estimated that pore pressure beneath the lower slope is close to lithostatic, while that beneath the upper slope is only slightly above hydrostatic. This result is consistent with the location of the highest rate of pore fluid expulsion from sediment thickening being beneath the lower slope [*Hyndman and Davis*, 1992]. The critical taper analysis assumed a friction coefficient of 0.85 on the decollement. If the coefficient is reduced beneath the lower slope by clays that have not been dehydrated, the result is the same, probable stable sliding behaviour. The shallow taper and inferred weak decollement extend to beneath the mid-slope, and this point thus may represent the seaward limit of the seismogenic zone. However, *Byrne and Fisher* [1990] have presented evidence that low friction and inferred high pore pressure extend to considerable depth beneath the accretionary wedge off Alaska (also discussion in Moore and Vrolijk, 1992). *Calvert and Clowes* [1991] have given seismic evidence for high pore pressures beneath the inner part of the Cascadia accretionary wedge.

At its most seaward end, the seismogenic zone includes a zone of conditional stability as elucidated by *Scholtz* [1990, p.320-321] that may have stable behaviour during the interseismic period, but unstable behaviour when triggered by slip in the seismically coupled zone. This conditional stability should move the seaward limit of the seismogenic zone a little further landward, although the exact amount is not clear.

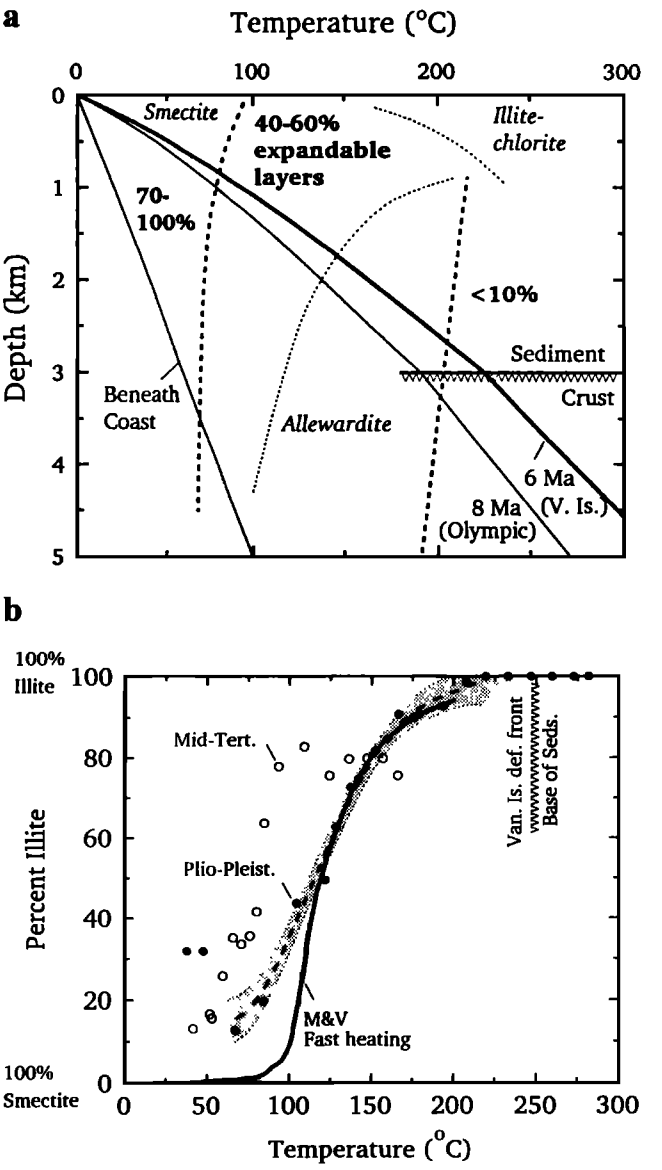

Fig. 5. (a) Progressive dehydration with increasing temperature for expandable clays that may exhibit stable sliding [from figure by *Chamley*, 1989, using data by *Velde*, 1985]. The percentages give the approximate amount of expandable smectite remaining. The geotherms at the deformation front off Vancouver Island (6 Ma) and off the Olympic Peninsula (8 Ma) (calculated as described in Appendix), and at the coast of Vancouver Island (from cross-section thermal model of Figure 7b) are shown for comparison. The zero depth is at the sediment surface.
(b) Progressive dehydration and transformation to illite clays with increasing temperature for Plio-Pleistocene [*Jennings and Thompson*, 1986] and Mid-Tertiary clastic sediments [*Hower et al.*, 1976], and the fast heating curve of *Moore and Vrolijk* [1992].

In the deformation modelling below, we have taken the seaward limit of seismogenic behaviour to be located beneath the lower slope where the frontal thrust faults reach the main sub-horizontal detachment, about 5 km landward of the deformation front. This limit is appropriate if expandable clay dehydration is the controlling factor. However, the limit could be substantially further landward as a consequence of high pore pressures and further study of this limit is certainly needed.

CALCULATION OF TEMPERATURES ALONG THE MEGATHRUST FAULT

The Modelling Procedure

Steady state thermal regimes are modeled for three profiles nearly perpendicular to the strike of the Cascadia subduction thrust zone (Figure 1). The cross section at Vancouver Island (Figure 6a) shows the basic geometry of the two-dimensional model. The oceanic plate covered with 3 km of sediment enters the model domain from the west (left) boundary with a specified convergence velocity v relative to the continental lithosphere, and exits the domain at the east (right) boundary, causing downward and landward convective transfer of heat. Heat transfer above the subducting plate is assumed to be purely conductive.

Neglecting heat carried by possible fluid motion and along-margin heat transport, the steady state temperature field T is described in a horizontal distance (x) and depth (z) coordinate system by

$$\left[\frac{\partial}{\partial x}\left(\lambda\frac{\partial T}{\partial x}\right)+\frac{\partial}{\partial z}\left(\lambda\frac{\partial T}{\partial z}\right)\right]-\left[\rho c\left(v_x\frac{\partial T}{\partial x}+v_z\frac{\partial T}{\partial z}\right)\right]+Q = 0 \qquad (3)$$

where Q is a source term that accounts for radiogenic and frictional heat, and ρc is the thermal capacity of the oceanic plate, the product of density ρ and specific heat c. The thermal conductivity λ, a function of x and z, is assumed to be isotropic and its dependence on temperature has been neglected since it is small compared to the other uncertainties. The first pair of square brackets encloses the conductive heat transfer term, and the second pair encloses the convective heat transfer term which is assumed to take place only in the subducting plate.

The upper surface of the model domain is kept at 0 °C, approximately the seafloor temperature, and the lower boundary at 1250°C, taken to be the basal temperature of the oceanic lithosphere at the depths as calculated in the appendix (see Figure A1). If vigorous thermal convection of asthenospheric material maintains the basal temperature of the oceanic lithosphere, the basal temperature will increase with depth following an adiabatic gradient of about 0.3 K km^{-1} [e.g., *McKenzie*, 1970; *Turcotte and Schubert*, 1982]. However, since the depth range of the model is only 80 km, a constant basal temperature with depth is an adequate approximation. At the east, inland end of the model, the horizontal heat flux across the vertical boundary is taken to be zero. This commonly used boundary condition is reasonable because the boundary is far from the region of interest, the seismogenic and transition zones of the megathrust. The temperatures at the left, seaward boundary of the model and the thickness of the incoming oceanic slab depend on the ocean floor sedimentation history, as well as on the age of the plate. A one-dimensional finite element model of a cooling lithosphere with a specified sedimentation history based on the theory developed by *Hutchison* [1985] is used to determine the temperatures and slab thickness, the details of which are described in the appendix. The sedimentation history is as given by *Davis and Hyndman* [1989]. The thermal conductivity λ and the thermal capacity ρc of the oceanic plate is taken to be 2.9 W m^{-1}K^{-1} and 3.3 x 10^6 J m^{-3}K^{-1}, respectively [see discussion in *Dumitru*, 1991]. The thermal conductivities for the different model units above the oceanic plate have been estimated from measurements on surface samples where available or taken from tables of typical values for the expected rock types as described below. The model structures are derived from the results of reflection and refraction seismic surveys described above.

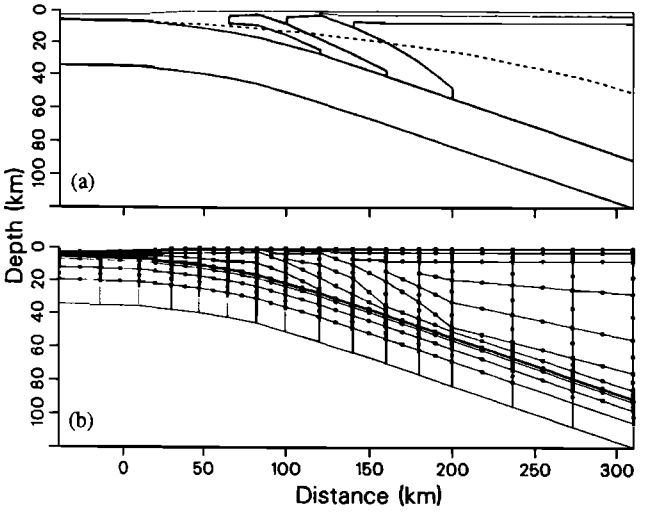

Fig. 6. (a) Simplified structural cross-section across the southern Vancouver Island margin as used in the thermal modelling. Thick solid lines define the geological units used in the model (see Figure 3 for the geological units); thin solid lines in the upper right portion divide the Wrangellia terrane into three heat generation sections. The upper surface of the oceanic plate for the Olympic Peninsula profile is plotted as a dashed line for comparison of plate geometry, (b) the finite element mesh.

Equation (3) with the above specified boundary conditions is solved numerically using a four-to-eight node isoparametric finite element model [*Bathe and Wilson*, 1976; *Wang*, 1989] for each of the three cross-sections. Within each element, the thermal property values are uniform but the temperature may vary quadratically. A layer of very thin elements (100 m) is used immediately below the surface to allow accurate calculation of surface heat fluxes.

Transient or steady state versions of equation (3) have been used to derive subduction zone thermal models by many authors [e.g., *Hasebe et al.*, 1970; *McKenzie*, 1970; *Minear and Toksoz*, 1970; *Anderson et al.*, 1978; *Sydora et al.*, 1978]. Recent systematic studies of subduction thermal models based on this equation have been conducted by *van de Beukel and Wortel* [1987, 1988] and *Dumitru* [1991] using numerical methods, and by *Molnar and England* [1990] using an analytical approach. The important question of sensitivity of the thermal regime to model parameters has been examined by *Dumitru* [1991]. He studied the effects of six subduction parameters, namely, subduction rate and angle, age of the subducting slab, thermal conductivity and heat generation within the forearc, and frictional heat along the plate contact. We do not repeat these general studies, but focus on the specific case of the Cascadia subduction zone where the first five of the six parameters are relatively well known through geophysical studies, especially at Vancouver Island. The parameter that remains poorly known is the amount of heat generation produced by friction between the two plates. This quantity has therefore been constrained in the model through fitting the surface heat flow data. The effect of varying the radioactive heat generation in the accretionary section has also been examined, although this parameter is reasonably well estimated by measurements on exploration well drill cuttings from the Vancouver Island shelf. The temperature at a particular point is approximately linearly dependent on the average thermal conductivity to that depth. Thus, the effect of varying this parameter is readily estimated without application to the numerical model. The calculated temperature distribution along the thrust

plane from the numerical model is used to estimate the downdip limits of the stick-slip seismogenic zone (350°C) and the stable sliding transition zone (450°C).

Discussion of Modelling Approach

Before describing the structure and parameters of each profile and presenting the model results, we discuss the modelling approach.

1. The importance of two-dimensional modelling. In the area of interest at the shallow portion of the subduction zone, the heat conduction above the thrust plane is almost vertical and hence nearly one-dimensional, because of the small angles of the megathrust detachments. A one-dimensional extrapolation of the geothermal gradient from the surface, using the surface heat flux and estimates of the thermal conductivity and heat generation rate within the upper plate [*Lewis et al.*, 1988; *Hyndman et al.*, 1989; *Davis et al.*, 1990], thus gives a good approximation of the temperature distribution along the thrust plane. However, two-dimensional modelling provides important additional information: (1) It allows an understanding of the effects of the various physical and thermal parameters on the thermal regime, i.e., the thrust geometry, the convergence rate, the age of the incoming oceanic lithosphere, and the magnitude of the frictional heating; (2) The models constrained by data, particularly surface heat flow, in some limited areas, can be used to predict the thermal regime in other areas where such data are not available.

2. Steady state in the upper plate. In this study we have ignored the thermal effects of sediment accretion. Different patterns of deformation result in different advective heat transfer within the wedge [*Wang and Shi*, 1984; *Barr and Dahlen*, 1990; *LePichon et al.*, 1990]. Recent work [*K. Wang et al.*, Thermal effects of sediment thickening and fluid expulsion in accretionary prisms: model and parameter analysis, submitted to *Journal Geophysics Research*, 1992] has shown that sediment thickening and fluid expulsion have an important effect on the deep temperatures in this area, but only in a restricted area extending for several 10s of km inland of the deformation front. There is a negligible effect in the area of interest, the landward limit of the seismogenic zone 50 to 150 km from the deformation front. *Le Pichon et al.* [1990] has shown that the effect of seaward advance of the deformation front is probably negligible. The approximation of steady-state in the upper plate is responsible for an important uncertainty in our model results, but the general agreement between the model temperatures within the accretionary prism and those from simple one-dimensional temperature estimates where there is good surface heat flow control, suggests that the errors in thrust plane temperatures from this approximation are small.

3. Adiabatic heating of the subducting slab and the thermal effects of metamorphic reactions are assumed to be negligible. Adiabatic heating may be ignored because of the small depth range of our problem [*Minear and Toksoz*, 1970; *Turcotte and Schubert*, 1982]. Heat produced or absorbed during metamorphic reactions in the oceanic crust or the overlying sediments have been discussed by a number of authors [e.g., *Anderson et al.*, 1976; 1978; *Minear and Toksoz*, 1970; *Gomshei et al.*, 1990; *Lewis et al.*, 1988], but the fit of our model result to surface heat flow data without such effects suggests that they are not important for this accretionary wedge area; they may be important at greater depth downdip. We follow *van de Beukel and Wortel* [1987, 1988], *Molnar and England* [1990], and *Dumitru* [1991], and do not include these processes in our models.

VANCOUVER ISLAND PROFILE

The southern Vancouver Island profile (Figure 1) follows multichannel reflection line 85-01 offshore and LITHOPROBE reflection line 84-01 across Vancouver Island [*Hyndman et al.*, 1990], extending a total of 350 km from 40 km seaward of the deformation front to a few tens of km seaward of the volcanic front. The geological units of the model section (Figure 6a) are constrained by the geophysical data described above. The present subduction rate of the Juan de Fuca plate relative to the American plate is about 45 mm yr^{-1}, which has changed little since the Eocene [*Riddihough*, 1984; *Engebretson et al.*, 1985; *Stock and Molnar*, 1988]. The convergence is nearly orthogonal at southern Vancouver Island compared to about 30° oblique off Washington and Oregon. For the Vancouver Island profile, the incoming oceanic plate was created at 6 Ma at the Juan de Fuca ridge approximately 250 km west of the coordinate origin of the model. Sedimentation mainly in the past 4 m.y. has accumulated a layer about 3 km thick. Figure 6b shows the finite element mesh. The thickness and the vertical temperature profile within the oceanic plate, both depending on the sedimentation history, are calculated using the procedure described in the appendix. The calculated temperature-depth profile in the sediment column just seaward of the deformation front is given in Figure 5a. The temperature at the top of the incoming oceanic crust at the deformation front is 250°C; this high temperature emphasizes that models taking the initial surface temperature of the downgoing plate to be 0°C can be seriously in error. The conductivity distribution for the accreted sediment has been derived from mineralogy data and porosity empirically determined from seismic velocity data [e.g., *Davis et al.*, 1990]; the conductivity values increase downward following the estimated decrease in porosity. In the model, each element in this terrane is assigned a uniform conductivity equal to the average for the depth range of the element. For each of the older terrains, namely Crescent, Pacific Rim and Wragellia, a uniform conductivity value is used (Table 2). Radiogenic heat generation rates for different terrains were inferred primarily from data on surface samples [*Lewis and Bentkowski*, 1988]. The measured heat generation rates from samples of the Crescent and Pacific Rim terrains are small and they are taken to be zero; that of the sediment is taken to be 0.6 μW m^{-3} [*Lewis et al.*, 1988; T. Lewis, personal communication, 1991]. There is considerable uncertainty in the heat generation of the Wrangellia terrain [*Lewis et al.*, 1988], and three possibilities have been considered.

Heat flow data. The most important constraint on subduction thrust thermal models is surface heat flux data. A thin veneer of unconsolidated sediment on the continental slope off southern Vancouver Island facilitates profiles of heat-probe measurements,

TABLE 2. Thermal Properties for the Preferred Model of Vancouver Island Profile

Geological Unit	λ W $m^{-1}K^{-1}$	Q μW m^{-3}	ρc MJ $m^{-3}K^{-1}$
Sediment	1.0 - 2.0*	0.6	
Crescent	2.0	0.0	
Pacific Rim	2.5	0.0	
Wrangellia	3.0	0.1 - 0.4*	
Oceanic plate	2.9	0.0	3.3

* Varies with depth, see text.

The parameters λ, Q, and ρc, are thermal conductivity, radiogenic heat generation rate, and thermal capacity, respectively.

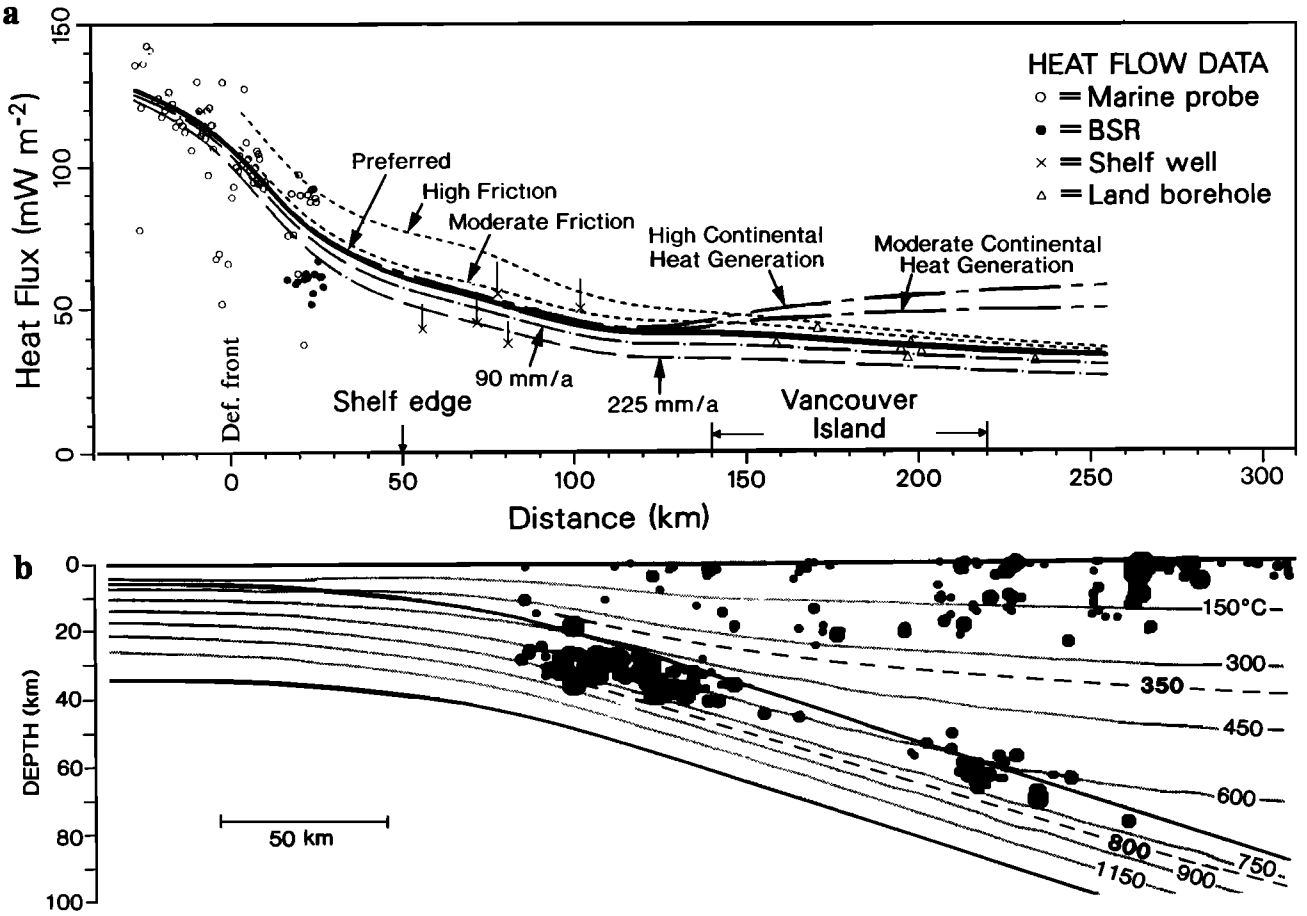

Fig. 7. (a) The calculated compared to observed heat flow on a profile across the Vancouver Island margin for models with the parameters in Table 2. Short dashed lines, high (α = 0.15) and moderate (α = 0.035) friction; Solid line, preferred model; dot-dash lines, higher convergence rates of 90 mm yr^{-1} and 225 mm yr^{-1}; long-short dash lines, moderate (model 2 in text), and high continental heat generation (model 3 in text).
(b) The subsurface temperature field on a profile across southern Vancouver Island predicted by the preferred thermal model with no frictional heating and low radioactive heat generation. A cross-section of seismicity across the margin through southern Vancouver Island is superimposed [after *Rogers et al.*, 1990].

whereas for many subduction zone accretionary wedges the seafloor sediments are generally too consolidated for probe penetration. The heat flux in the deep-sea basin and on the continental slope along the profile has been measured using a multipenetration marine probe [*Davis et al.*, 1990]. The data within 10 km of the profile of Figure 1 are shown in Figure 7a. On the continental slope, a bottom-simulating-reflector (BSR) that defines the thermally controlled base of the stability field for methane hydrate occurs on seismic records at a depth of about 200 - 300 m. *Davis et al.* [1990] have also estimated heat flux values from the depth of the BSR, and found values on the mid-slope that were slightly lower than the probe values (Figure 7a). Subsequent studies [K. Wang et al., Thermal effects of sediment thickening and fluid expulsion in accretionary prisms: model and parameter analysis, submitted to *Journal of Geophysical Research*, 1992] have shown that the effect of sediment thickening and fluid expulsion is restricted to a zone extending about 30 km inland from the deformation front. The heat flow data from this zone thus have not been used as a model constraint. The measured heat flux is also affected by sedimentation which tends to counter balance the effect of fluid expulsion. The magnitude of this latter effect is poorly constrained but it is estimated it to be small. We have used mainly the probe heat flux measurements offshore and the land borehole measurements onshore for the model constraint, noting that there is a probable uncertainty of $\pm$15% in the marine data and $\pm$5 to $\pm$10% in the land data.

Heat fluxes on the shelf were determined from hole-bottom temperatures and thermal conductivity estimates from petroleum exploration wells [*Lewis et al.*, 1988; *Lewis*, 1990]. Rough corrections have been applied to the temperatures for drilling disturbance, but the estimated gradients have an uncertainty of about $\pm$15%. Thermal conductivities were estimated from measured grain matrix conductivities using well cuttings and porosity estimates from down-hole logs [*Lewis et al.*, 1991]. The earlier reported conductivity values have been found to have a systematic error as discussed by *Lewis et al.*, [1991], and revised values 20% higher are now suggested (bar extensions of data points in Figure 7a). Numerous heat flux measurements have been made in land boreholes that are believed to be very reliable [*Lewis et al.*, 1988; 1992]. Additional measurements have been made in the deep coastal inlets using the ocean probe technique that give results consistent with the borehole data [e.g., *Lewis et al.*, 1988]. The continental data within 100 km of the profile of Figure 1 are shown in Figure 7a. The heat flow pattern exhibits

a smooth decrease landward from values of about 120 mW m^{-2} in the Cascadia Basin to 80 on the mid-slope, 60 on the shelf and 40 on Vancouver Island. For modelling constraints, the marine probe measurements along the profile have been combined with the land data within 100 km of the profile that have been projected onto it (Figure 7a).

The preferred model. A range of model parameters have been tried to determine which values give results agreeing with the major constraint of surface heat flow. We first consider cases in which frictional heating is ignored. Three heat generation models for the Wrangellia terrain are considered (Figure 7a); surface sample data indicate an average of about 0.6 μW m^{-3}: (1) three layers with heat generation decreasing from the surface, with values of 0.6, 0.4, and 0.1 μW m^{-3}; (2) a uniform value of 0.6 μW m^{-3}; and (3) a uniform value of 0.8 μW m^{-3}. The calculated heat fluxes seaward of the shelf edge are insensitive to the Wrangellia heat generation and agree very well with the trend of the measured values. Model 1 with the lowest average heat generation best fits the land heat flux data (Figure 7a), and hence is accepted as the preferred model. We estimate that the temperatures for the thrust plane in the region of interest from this model have an uncertainty of about $\pm$25°C.

A comparison of the subsurface temperature field and the seismicity cross section for the Vancouver Island profile (Figure 7b) shows good correspondence between the maximum depth of earthquakes and the stick-slip to stable sliding transition estimated to be at 350°C for crustal rocks (as discussed above) and about 800°C for mantle rocks [e.g. *Wiens and Stein,* 1983]. The earthquakes are from a careful relocation of well recorded events from 1982 to 1989 within a 30 km wide corridor centred along the profile [*Rogers et al.*, 1990]; the events plotted are restricted to those with an uncertainty in depth of less than $\pm$5 km. The maximum depth of earthquakes in the overlying continental crust (i.e., for crustal rocks) along the profile is seen to be about 300°C and the maximum for the Benioff-Wadati earthquakes within the downgoing plate (i.e., for mantle rocks) is approximately 800°C.

The temperature distributions as a function of distance along the thrust plane for the various models are plotted in Figure 8; the preferred model as a solid line. Taking the downdip temperature limits of the stick-slip seismogenic and stable sliding transition zones as 350°C and 450°C respectively, and the seaward limit of the seismogenic zone to be where the frontal thrust merges to the megathrust plane as discussed previously, the length of the seismogenic zone for the preferred model is about 40 km and the transition zone about 60 km. The whole seismogenic zone is beneath the continental slope and the transition zone extends landward to under the inner shelf (Figure 1).

Frictional heating. The agreement between the preferred model results and the measured surface heat flux values (Figure 7a) appears to exclude significant frictional heating on the thrust detachment to a depth of at least 40 km. However, as noted below, frictional heating may be important for other colder subduction zones that subduct older oceanic lithosphere. We provide a simple analysis of frictional heating to illustrate the expected pattern with landward distance. The amount of frictional and shear heating q is proportional to the absolute shear stress τ which is poorly known, for the following reasons. (1) The magnitudes of shear stress on plate boundaries, remain controversial; estimates range from less than 10 MPa to over 100 MPa [e.g., *Turcotte and Schubert,* 1982; *Lachenbruch and Sass,* 1980]. (2) The effective normal stress σ^* is reduced by pore fluid pressure which is commonly interpreted to be high in accretionary prisms. High pore pressure beneath the lower slope area is discussed above and exploration wells into Tofino basin that overlies the accretionary wedge on the shelf have reported pore pressures close to lithostatic [*Shouldice,* 1971]. (3) The location and nature of the transition from a friction law rheology at shallow depths to power law rheology at greater depths is not known. These now appear to be better known for major transform boundaries [*Lachenbruch and Sass,* 1992] but are poorly known for subduction zones.

We adopt the simple method of *van de Beukel and Wortel* [1987; 1988] to obtain very rough estimates of frictional heating. The heat generation rate by friction in a narrow zone with width w is

$$q = v\tau/w. \qquad (4)$$

Experimental constants for the power-law rheology of wet quartzite [*Koch et al.*, 1980] are used for the ductile portion of the fault. Because of the uncertainties in the magnitudes of shear stress and of the pore pressure for the portion of the thrust plane where the friction law is applied, *van de Beukel and Wortel* [1987, 1988] used an *ad hoc* relation between shear stress and lithostatic pressure:

$$\tau = \alpha \rho g z \qquad (5)$$

where g is gravity, ρ is density, and α is a constant. The change from the friction law to the power law was prescribed by them to be at a depth of 40 km. The parameter α was chosen to maintain shear stress continuity at this point. To apply this method to our model, we must assume that the change from friction law to power law occurs somewhere in the stable sliding transition zone between temperatures of 350°C and 450°C. The two extreme cases have been calculated with the change of rheology taking place, (1) at 350°C and (2) at 450°C, using the temperatures given by the preferred model. The constant α was determined to be 0.15 and 0.035 for the two cases, respectively. The calculated surface heat flux for these two cases are shown in Figures 7a and the temperature distributions along the thrust plane are plotted in Figure 8 for comparison with that of the preferred model.

Introduction of such frictional and shear heating results in calculated surface heat fluxes that are significantly higher than observed; while spatial distributions of model parameters can be found that allow significant frictional heating and give the observed heat fluxes, the parameter values required are beyond the reasonable range. This result demonstrates that frictional heating is probably unimportant in this area. In the computation described above, most of the heat was generated in the portion of the fault that obeys the friction law. Thus, for colder subduction zones with older or faster underthrusting oceanic lithospheres, the portion of the thrust plane obeying the friction law will extend to greater depths and frictional heating will be more important. In the study of *Hasabe et al.* [1970] the observed low heat flow in the Japan forearc could be modelled only with frictional heating restricted to depths greater than 60 km. Off southern Mexico where young oceanic lithosphere is also being subducted, *Ziagos et al.* [1985] also found that to model the low margin heat flow, significant frictional heating must be restricted to depths greater than 70 km. In summary, frictional heating seems negligible in the Cascadia subduction zone, although it may be important elsewhere. If frictional heating were large, its effect would be to move the 350 and 450°C isotherms upward, resulting in narrower and more seaward seismogenic and transition zones (Figure 8).

Faster convergence. The convergence rate is an important parameter defining the temperature limits of the seismogenic and transition zones. The temperature fields have been computed for

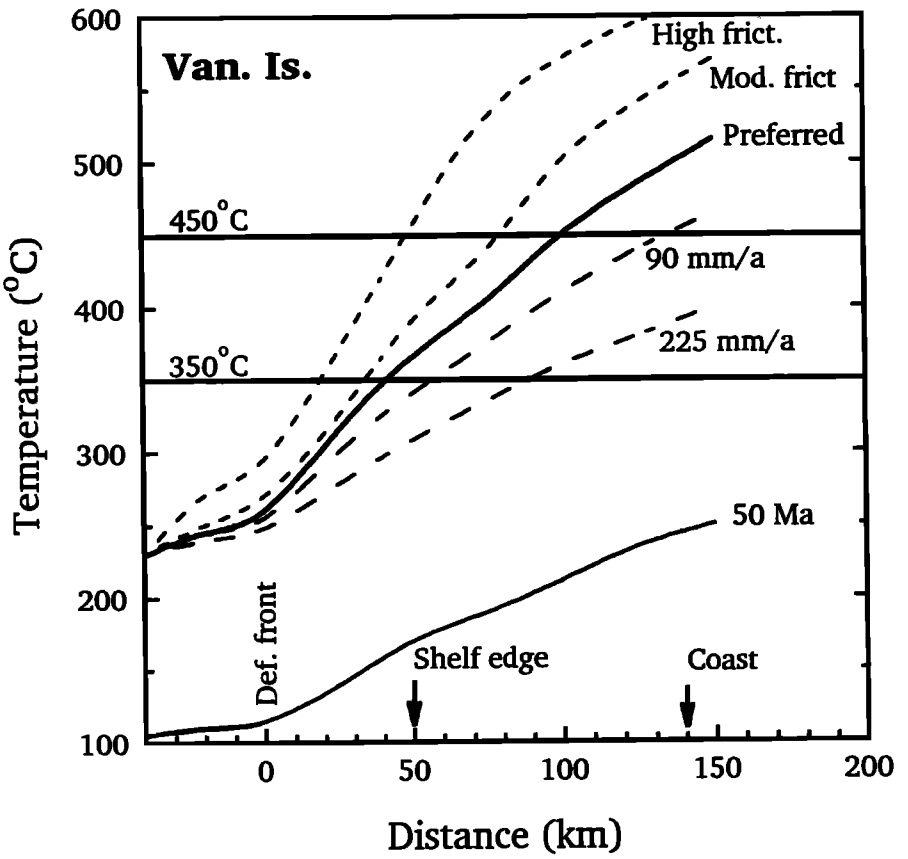

Fig. 8. The temperature distribution landward along the main thrust plane as a function of horizontal distance from the deformation front on the southern Vancouver Island profile, for models with the parameters in Table 2. Dashed lines, very high (α = 0.15), and moderate (α = 0.035) friction; Solid line, preferred model; dot-dash lines, higher convergence rates of 90 mm yr^{-1} and 225 mm yr^{-1} ; long-short dash line, 50 m.y. age incoming ocean crust. The 350 and 450°C limits to the stick-slip and transition zone are shown. The 90 mm yr^{-1} curve approximates that for the Chile margin at the location where the oceanic crust has a similar age to off Vancouver Island.

this margin with rates double (90 mm yr^{-1}) and 5 times (225 mm yr^{-1}) the Cascadia value, and the other parameters the same as in the preferred model. It is seen that for faster convergence, the surface heat flow (Figure 7a) is lower and the seismogenic and transition zones of the megathrust (Figure 8) are much wider. This is in agreement with the inference from the compilation by *Ruff and Kanamori* [1983] showing that subduction zones with faster convergence tend to have larger earthquakes. The relatively slow convergence rate is one of the factors contributing to the unusually high temperatures and shallow seismogenic zone on the Cascadia margin, however, it is less important than the young age of the incoming oceanic plate and the thick insulating sediment cover.

Older oceanic plate. Based on the thermal constraints alone, an older (50 Ma) oceanic plate, because it is cooler and thicker, results in a stick-slip zone that extends very much further landward (Figure 8). The thickness and vertical temperature profile of such an incoming plate was calculated using the procedure described in the appendix. All parameters except those related to plate age are the same as for the preferred model. Much wider seismogenic zones and hence potentially larger maximum magnitude earthquakes result from such models. We note that this is contrary to the inference from the compilations of *Ruff and Kanamori* [1983] [also *Kanamori*, 1986] that subduction zones with younger subducting plates tend to have larger megathrust earthquakes. If their association is correct, other factors than the thermal regime must be important in controlling the maximum earthquake size.

APPLICATION TO OTHER AREAS

Olympic Peninsula Profile

The agreement between the calculated surface heat fluxes of the preferred model of the Vancouver Island profile and the observed values indicates that the modelling approach, boundary conditions, and parameter values, are probably good approximations. With similar model parameters we can estimate the thermal regimes for the other two profiles shown in Figure 1 where there are fewer surface heat flux measurements and less structure data to provide model control. The Olympic profile has an added complication in the thermal effect of the rapid erosion of the exposed accretionary wedge sediments on the Olympic Peninsula. However, since the critical region is mainly seaward of the margin we have not included erosion in our model.

The structure for the Olympic cross section in the region where the thrust may be seismogenic is relatively simple, the accreted sediments extending well landward of the coast; the core of the Olympic Peninsula consists of accreted sedimentary rocks. For nearly the total length of the profile the hanging wall of the thrust fault must be accreted sediments [e.g., *Snavely*, 1987]. The

important contrast with the Vancouver Island profile is that the dip angle of the thrust fault across the Olympic margin is very much shallower. We have used the plate geometry shown in *Davis and Hyndman* [1989] defined primarily by the Benioff-Wadati seismicity [*Crosson and Owens,* 1987], and have assumed that the thrust detachment is at the top of the oceanic crust, although this is not well established by the available seismic data. The upper boundary of the subducting plate is plotted as a dashed line in Figure 6a. The oceanic plate is 8 m.y. old at the deformation front and consequently the plate is slightly thicker and the incoming surface temperature is lower compared to the Vancouver Island margin (see appendix). The thermal conductivity of the sediment at the seaward end of the cross section has been taken to change with depth in the same fashion as for the Vancouver Island model, but it is also taken to increase with distance inland due to the consolidation and diagenesis of the sediments with increasing age.

Unfortunately, no conductivity measurements are available along the profile. The closest three land sites where conductivity was measured in the accretionary wedge were about 50 to 100 km south of the profile near the coast; the borehole average values reported by *Blackwell et al.* [1990] are 1.3, 1.5, and 2.0 W m^{-1} K^{-1}. We estimate the maximum conductivity of the sediment to be 2 W m^{-1} K^{-1}, and allow the surface conductivity to increase gradually inland to reach this value.

The predicted temperature distribution along the thrust plane is shown in Figure 9a. The model heat flux of the land portion of the profile is consistent with the limited available data [*Blackwell et al.*, 1990]. To test the sensitivity of the model results to the value of maximum sediment conductivity, we also generated models with maximum conductivities of 1.7 and 2.3 W m^{-1} K^{-1}. The temperatures are little different (Figure 9a). The radiogenic heat generation rate of the accreted sediments is taken to be a uniform 0.6 μW m^{-3} in the preferred model, but the effect of using a value of 0.4 μW m^{-3} was found to give very little difference in the thermal results. Using the temperature limits of 350°C and 450°C and the seaward limit defined by the frontal thrust, the stick-slip zone has a width of about 100 km beneath the continental slope and outer shelf, with the transition extending another 80 km landward to just inland of the coast. These positions for the two zones are markedly different from those for the Vancouver Island margin. We note that the widths of the locked and transition zones as modelled by *Savage et al.* [1991], 100 and 75 km respectively for the Olympic Peninsula, agree with our model. However, the agreement results from their use of the temperatures estimated for the Vancouver Island profile of *Davis et al.* [1990] which are much higher than calculated for the Olympic profile, and a higher seismogenic temperature limit of

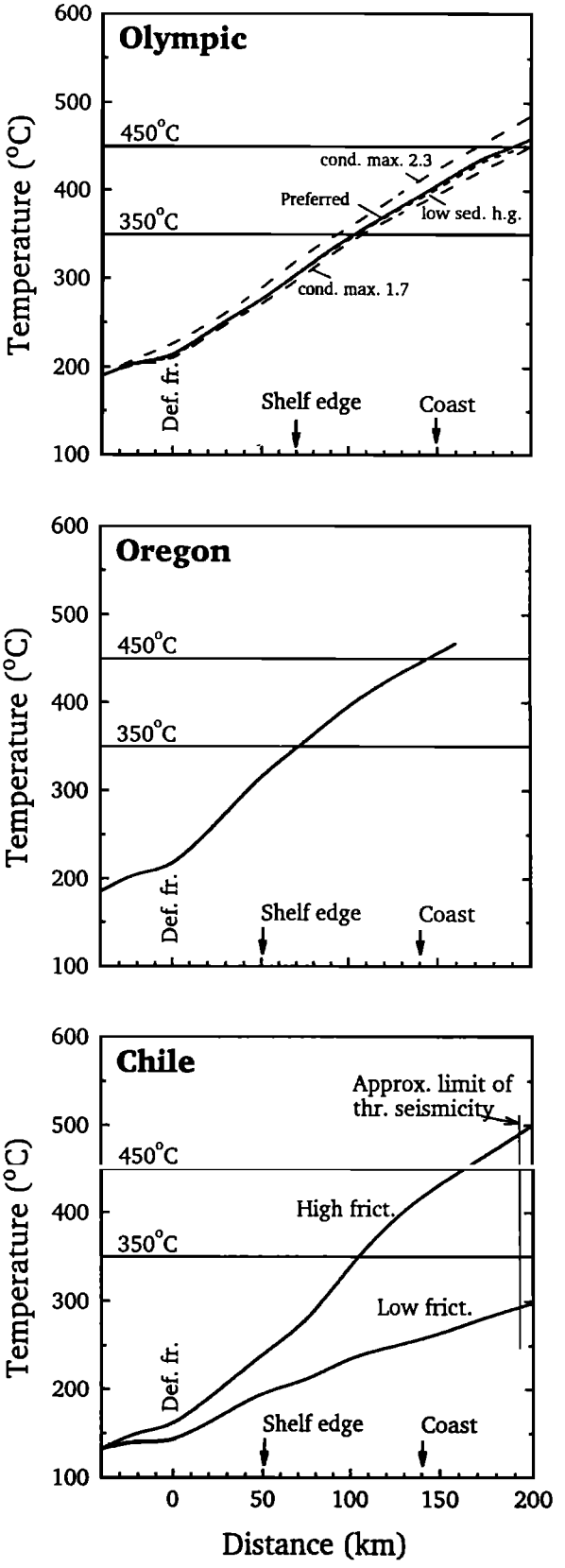

Fig. 9. (a) The temperature distribution landward along the main thrust plane as a function of horizontal distance for the Olympic Peninsula profile. Solid curves, sediment heat generation of 0.6 μW m^{-3} with maximum sediment conductivity of 2.0 (thick curve, preferred), 2.3 (upper) and 1.7 (lower) W $m^{-1}K^{-1}$. Dashed curve, sediment heat generation of 0.4 μW m^{-3} and conductivity of 2.0 W $m^{-1}K^{-1}$.
(b) The temperature distribution landward along the main thrust plane as a function of horizontal distance for northern Oregon. The plate geometry and model parameters are the same as for the Vancouver Island profile (Table 2), but with plate age of 8 Ma.
(c) The temperature distribution landward along the main thrust plane as a function of horizontal distance for a model with the structure and parameters of Vancouver Island, but with the oceanic plate age and convergence rate at the central Chile (20 Ma) profile. The lower curve is for no frictional heating and the upper curve for large frictional heating as described in text. The approximate thrust seismicity limit for that portion of the Chile margin from *Tichelaar and Ruff* [1991] is shown for comparison.

450°C rather than 350°C. Here we provide a more complete physical explanation for the limits.

Oregon Profile

We have not attempted to model the details of the structure across the Oregon margin, but have for comparison used a structure similar to that for the Vancouver Island margin. The structure of the land portion of the Oregon cross-section is not well constrained by seismic data, but the offshore accretionary wedge structure is similar to that off Vancouver Island. The important exception noted above is that on some marine seismic sections off Oregon, the detachment at the deformation front is above the oceanic crust within the sediment section [*MacKay et al.*, 1992]. If the thrust surface remains at this level in the subducted section above the downgoing oceanic crust, the seismogenic zone may extend several tens of kilometres further landward than in our model results. We use the same parameter values as for the preferred model of the Vancouver Island profile (Table 2); the only changes are adjustments to the thickness and temperatures of the incoming oceanic plate according to its age of 8 Ma.

Off Oregon there is a series of heat probe measurements on the continental slope reported by *Shi et al.* [1988]. While the detailed variations are controlled by the fold and thrust configuration, the overall pattern is very similar to that off Vancouver Island.

The predicted temperatures along the thrust plane are shown in Figure 9b. We estimate that both the seismogenic and transition zones for off Oregon are about 70 km wide. We note that the width to the 450°C landward limit given by *Blackwell* [1991] is narrower. He obtained higher temperatures, assuming that the low thermal conductivity Crescent basalts that outcrop on the coast extend downward to the oceanic plate, rather than being a thin sliver as interpreted from seismic data off Vancouver Island.

Other Subduction Zones

A critical confirmation of the constraints on the seismogenic zone provided by thermal models is comparison with actual thrust earthquake data. This requires detailed modelling of other margins where major thrust earthquakes have occurred, which is beyond the scope of this article. However, we first show the consequences of parameters characteristic of other subduction zones that are very different from those for the Cascadia margin. Second, we provide one comparison of the seismogenic zone estimated from thermal constraints, with the position from earthquake data, taking the example of the central Chile margin.

The important parameters that result in an atypical thermal regime on the Cascadia margin are, (1) young and thus hot subducting oceanic crust, (2) thick insulating sediment section on the incoming seafloor, and (3) slow subduction rate. The sensitivity to each of these parameters is illustrated above for the Cascadia margin (Figure 8).

1. A model with an older, 50 m.y. old incoming plate but the other parameters the same as those for the preferred Vancouver Island margin model, gives the position of the critical 350°C isotherm more than 200 km inland of the deformation front (Figure 8), where the downgoing plate is over 50 km deep. However, the assumption of negligible frictional heating is unlikely to be valid to this depth for such a cold thrust plane and the 350°C isotherm is undoubtedly reached at a shallower point as evident from the frictional heating model results of Figure 8.

2. The effect of little or no sediments along this profile is to reduce the initial temperature of the thrust at the deformation front from 250 to near 0°C, and thus extend the locked zone to a distance of approximately 200 km landward of the deformation front. Again the neglect of frictional heating in the preferred model makes this a maximum distance.

3. Finally, increasing the subduction convergence rate by a factor of five, from 45 to 225 mm yr^{-1} extends the locked zone to about 90 km landward of the deformation front (Figure 8).

Thus, the effect of varying these three parameters to values that are common in other subduction zones is large; for most subduction zones the predicted locked and transition zones are much wider than for Cascadia.

Chile margin. For a more specific comparison we have chosen a section across the margin of central Chile where there is good earthquake data [e.g., *Tichelaar and Ruff*, 1991]. We take a profile near latitude 37°S, where the sediment thickness and plate geometry are similar to the Vancouver Island profile [e.g., *Spence*, 1989]. We have not modelled this margin exactly, but have kept the geometry and thermal parameters identical to those for the Vancouver Island section. The differences are older incoming plate, about 30 Ma, and a faster convergence rate, about 90 mm yr^{-1}. The results for a case without frictional heating and a case with very large frictional heating are given to represent a reasonable range.

The modelling results from the colder older plate and the more rapid convergence rate show the locked zone to be very much larger, extending landward of the deformation front to at least 250 km from the deformation front for no frictional heating, and 110 km for the very high frictional heating case (Figure 9c). The high heating case predicts quite high heat flow in the forearc region, inconsistent with the available data on the margin just to the south [*Cande et al.*, 1987]. The true value probably lies between these two extremes, i.e., 150 to 200 km where the thrust is at a depth of about 50 km. While we emphasize that this is not a rigorous thermal model for the Chile margin, these results encompass the maximum landward extent of thrust seismicity in this region (about 50 km depth) from *Tichelaar and Ruff* [1991].

To the south along the Chile margin near 44° S, the age of the incoming crust is similar to off Vancouver Island, but the convergence rate is about double [*Cande et al.*, 1986]. Assuming that the structure and plate geometry are similar to that off Vancouver Island, the seismogenic zone is estimated to be about 60 km wide and the transition zone another 80 km landward (Figure 8). The structure and tectonic regime are complex because a spreading ridge intersects the margin just to the south. However, these widths give approximately the observed coseismic displacement profile observed as discussed in the next section.

To confirm this general agreement, more complete modelling is needed on margins where there is good thrust seismicity data and enough surface heat flow data for good constraint on the magnitude of frictional heating.

DEFORMATION PREDICTED BY DISLOCATION MODELS

Although we do not discuss contemporary deformation data in detail, it is important to compare observed interseismic horizontal and vertical strains with those predicted by our models. *Savage et al.* [1991] showed for a section across the Olympic margin that a locked zone 100 km wide under the outer shelf and a transition zone extending 75 km further inland, similar to our results, gave predicted deformation in good agreement with both the horizontal and vertical contemporary deformation data. A number of sophisticated models for the subduction zone earthquake cycle have been developed [e.g., *Melosh and Raefsky*, 1983; *Thatcher*

and Rundle, 1984; *Stuart,* 1988]. However, to predict the deformation during the interseismic period, we employ only the simple model of an edge dislocation in an elastic half-space provided by *Savage* [1983] (Figure 10).

Dislocation Models

In the simple dislocation representation of earthquakes, the shallow seismogenic portion of the plate interface remains locked until sufficient stress has accumulated to cause failure. The abrupt motion recovers the accumulated slip deficit and that portion of the fault zone immediately re-locks. In the model of *Savage* [1983], at some distance downdip there is continuous slip throughout the earthquake cycle at the plate convergence rate. During the interseismic period, the steady slip rate decreases upward through a transition zone to zero at the downdip end of the locked zone. When the locked zone fails, the abrupt motion extends beyond the locked zone with decreasing displacement downdip to zero at the landward end of the transition zone. Short term pre- and post-seismic slip are included in the main abrupt event. The strain accumulation and deformation rate are also assumed to be constant through the interseismic period.

To calculate the interseismic deformation rates, the thrust zone is divided into the locked zone where the slip deficit accumulates at the plate rate, a transition zone where the slip deficit decreases downdip from the full plate rate to zero, and the remainder where no slip deficit accumulates. The portion of the fault zone seaward of the locked zone, where there is stable sliding behavior but motion only occurring during earthquakes, is included in the locked zone. Its effect will be small for measurements in the adjacent coastal region. In the dislocation models we take a planar geometry with dip equal to that near the landward end of the locked zone. The locked zone on each profile extends downdip to where the thermal model temperature is 350°C and the transition zone to extend to 450°C. We take the fault to extend seaward to the seafloor. The deformation predicted for locked zones 15 km narrower and 30 km wider than the preferred models have also been computed to illustrate a reasonable uncertainty range (Figure 11). The irregularity of the horizontal strain plot is a consequence of constraining the steady interseismic slip within the transition zone to vary exactly linearly downdip from zero to the full plate rate.

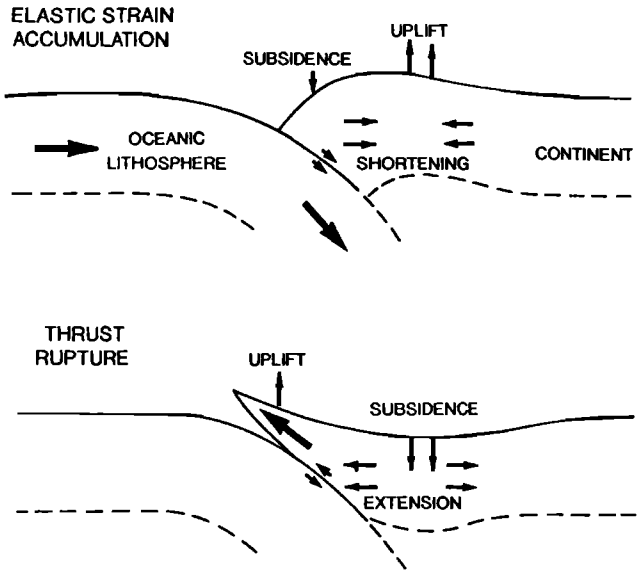

Fig. 10. Schematic diagram showing the directions of horizontal and vertical deformation, for the period of interseismic strain accumulation and for the seismic rupture.

Geodetic and Tide Gauge Data

We compare the predicted interseismic deformation from the dislocation model with two types of contemporary data, crustal shortening from repeat geodetic measurements and vertical motion from continuous tide gauge recordings. The crustal shortening data is listed in Table 3 and the comparison with the predictions in Figure 11. The Alberni network (H. Dragert, personal communication, 1991) which is close to the southern Vancouver Island profile, has a very oblique shortening direction that may reflect the effect of the 3-dimensional corner in the coastline. The Juan de Fuca Strait geodetic network [*Lisowski et al.,* 1989] is between the southern Vancouver Island and Olympic Peninsula profiles and is included on both plots; the Olympic and Seattle networks [*Savage et al.,* 1991] and Bellingham network [*Snay and Matsikari,* 1991] are close to the Olympic Peninsula profile; and the Portland network [*Snay and Matsikari,* 1991] and Columbia network (M. Lisowski, personal communication, 1991) are close to the Oregon profile.

Except for the Olympic and Seattle networks, the geodetic data are currently unable to resolve all three independent components of the horizontal strain rate tensor. The values of maximum shortening in the principle direction in Table 3 are based on the assumption of uniaxial shortening for the other networks. Such an assumption is supported by evidence for contemporary compression rather than extension parallel to the margin [e.g., *Spence,* 1989]. Other assumptions on the strain rate will lead to different maximum shortening values. For example, assuming pure shear strain will reduce the values by half. In Figure 11, if the maximum shortening values have directions more than 10° from the direction of the profiles, they have been resolved onto the directions of the profiles.

While the data uncertainties are large, there is observed shortening across the margin in all surveys as predicted and the agreement between the predicted and observed magnitudes of crustal shortening is generally good. The Juan de Fuca survey which lies between the Vancouver Island and Olympic profiles gives values of shortening between that modelled for the two profiles as expected. The observed magnitudes of shortening appear to exclude a locked zone that extends to the coast or further inland, if strain is accumulating at the plate convergence rate.

Contemporary sealevel trends from tide gauge data have been provided by *Wigen and Stephenson* [1980] (see *Riddihough* [1982] and *Clague et al.* [1982] for discussions) for the southern British Columbia coast and by *Hicks* [1978] (see *Savage et al.* [1991] for discussion) for the Washington and northern Oregon coast. For the southern Vancouver Island margin sites, we have employed the recent results of G.C. Rogers (Vertical motion in the Vancouver Island region of the Cascadia subduction zone, unpublished manuscript, 1991) who analyzed additional data, employed monthly rather than yearly means, and reduced the atmospheric and oceanographic effects by taking differences from a well determined reference station. We present data only from the more reliable stations with a minimum of 30 years of recording. *Ando and Balazs* [1979] and *Holdahl et al.* [1989] have also provided a regional distribution of uplift and subsidence that are consistent with the individual tide gauge results for the area, integrating both tide gauge and repeat survey levelling.

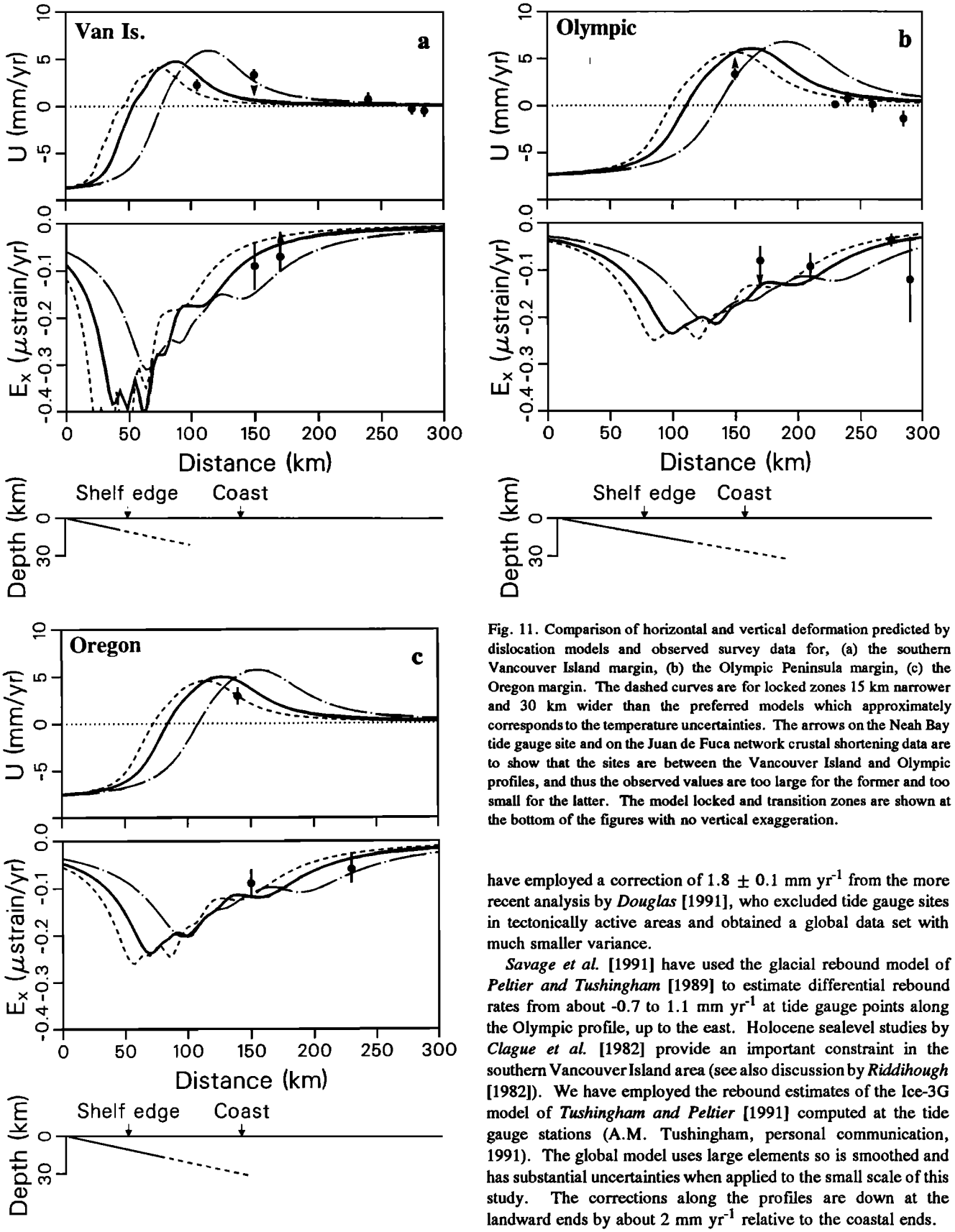

Fig. 11. Comparison of horizontal and vertical deformation predicted by dislocation models and observed survey data for, (a) the southern Vancouver Island margin, (b) the Olympic Peninsula margin, (c) the Oregon margin. The dashed curves are for locked zones 15 km narrower and 30 km wider than the preferred models which approximately corresponds to the temperature uncertainties. The arrows on the Neah Bay tide gauge site and on the Juan de Fuca network crustal shortening data are to show that the sites are between the Vancouver Island and Olympic profiles, and thus the observed values are too large for the former and too small for the latter. The model locked and transition zones are shown at the bottom of the figures with no vertical exaggeration.

Two corrections must be considered to the sealevel trends, global eustatic sealevel change, and local glacial isostatic rebound. *Holdahl et al.* [1989] used a eustatic correction of 1.2 mm yr^{-1}. *Savage et al.* [1991] used an correction of 2.4 ± 0.9 mm yr^{-1} from the global analysis by *Peltier and Tushingham* [1989]. We have employed a correction of 1.8 ± 0.1 mm yr^{-1} from the more recent analysis by *Douglas* [1991], who excluded tide gauge sites in tectonically active areas and obtained a global data set with much smaller variance.

Savage et al. [1991] have used the glacial rebound model of *Peltier and Tushingham* [1989] to estimate differential rebound rates from about -0.7 to 1.1 mm yr^{-1} at tide gauge points along the Olympic profile, up to the east. Holocene sealevel studies by *Clague et al.* [1982] provide an important constraint in the southern Vancouver Island area (see also discussion by *Riddihough* [1982]). We have employed the rebound estimates of the Ice-3G model of *Tushingham and Peltier* [1991] computed at the tide gauge stations (A.M. Tushingham, personal communication, 1991). The global model uses large elements so is smoothed and has substantial uncertainties when applied to the small scale of this study. The corrections along the profiles are down at the landward ends by about 2 mm yr^{-1} relative to the coastal ends.

We present the eustatic and glacial loading rebound corrected uplift rates from the tide gauge data in Table 4. Five sites are within 50 km of the southern Vancouver Island profile, 6 sites within 50 km of the Olympic profile and one on the Oregon profile. As for the shortening data, the agreement with the dislocations model predictions is generally good (Figure 11). The

Neah Bay tide gauge station, like the Juan de Fuca geodetic network, lies between the Vancouver Island and Olympic model profiles and is included on both plots. Thus, as with the geodetic data, the uplift is greater than that from the Vancouver Island model and less than from the Olympic model. An important conclusion from the consistent positive uplift at the most seaward sites is that the locked zone must be well offshore on all of the profiles; in our dislocation model results the hinge point with uplift landward and subsidence seaward is just landward of the end of the locked zone.

Some additional confirmation of the thermal modelling results comes from a comparison of the coseismic vertical motion predicted by the dislocation model for southern Chile where the ocean crustal age is similar to that off Vancouver Island, and that observed by *Plafker and Savage* [1970] for the large 1960 earthquake. They found the hinge line between uplift and subsidence to be located about 90 km inland of the deformation front. The Vancouver Island model with a 90 mm yr^{-1} convergence rate (Figure 8) predicts 75 km. However, the dip angle at this location on the Chile margin, although not well constrained, appears to be shallower [*Tichelaar and Ruff*, 1991] perhaps closer to that of the Olympic profile. With the Olympic dip angle and the slightly younger age estimated for the Chile profile, the predicted hinge line is about 95 km from the deformation front. Thus, the hinge line predicted from thermal modelling and that from the coseismic vertical motion agree within the uncertainties. Detailed models for the Chile margin are needed to confirm this agreement.

TABLE 3. Summary of Geodetic Data for Crustal Shortening Across the Cascadia Margin

Network	Distance From Deformation Front, km	Strain Rate, μstrain yr^{-1}	Direction of Maximum Shortening	Ref.
Alberni	150 Van. Is.	0.06±0.03	N 18° E±11°	(5)
Juan de Fuca	170 V Is & Oly	0.09±0.03	N 82° E±8°	(2)
Bellingham	290 Olympic	0.12±0.09	N 71° E±21°	(3)
Olympic	210 Olympic	0.09±0.03	N 59° E±7°	(1)
Seattle	275 Olympic	0.04±0.01	N 68° E±6°	(1)
Portland	230 Oregon	0.06±0.03	N 95° E±14°	(3)
Columbia	150 Oregon	0.09±0.03		(4)

From (1) *Savage et al.* [1991]; (2) *Lisowski et al.* [1989], (3) *Snay and Matsikari* [1991], (4) M. Lisowski (personal communication, 1991), (5) H. Dragert (personal communication, 1991). Except for the Olympic and Seattle networks, the strain rates shown in this table are based on the assumption of uniaxial shortening. The rates have been resolved in the direction of the profiles.

TABLE 4. Summary of Uplift Rates From Tide Gauge Data for Stations Along the Cascadia Margin

Site	Distance From Deformation Front, km	Sea Level Rate, mm yr^{-1}	Eustatic Uplift, mm yr^{-1}	Rebound Correction, mm yr^{-1}	Profile	Ref.
Vanc.	285	0.3±0.3	1.5±0.4	-0.5±0.6	VI	(1)
Point Atkinson	275	0.1±0.3	1.7±0.4	-0.3±0.6	VI	(1)
Fulford Harbour	240	0.1±0.4	1.7±0.5	0.7±0.7	VI,Oly	(1)
Tofino	105	-0.8±0.3	2.6±0.4	2.2±0.6	VI	(1)
Neah Bay	150	-1.5±0.3	3.3±0.4	3.3±0.6	VI,Oly	(2)
Victoria	230	0.7±0.1	1.1±0.2	0.1±0.4	Oly	(1)
Friday Harbour	260	0.6±0.5	1.2±0.6	0.1±0.8	Oly	(2)
Seattle	285	2.5±0.5	-0.7±0.6	-1.4±0.8	Oly	(2)
Astoria	140	-0.4±0.6	2.2±0.7	2.9±0.9	Oreg	(2)

From (1) G. C. Rogers (unpublished manuscript, 1991), (2) *Hicks* [1978] as cited by *Savage et al.* [1991] with small revisions by *Rogers* [1991].

CONCLUSIONS

We have examined the thermal limits to the seismogenic zone of the megathrust off the Cascadia margin. Four divisions of the thrust plane are defined: (1) a zone just landward of the deformation front that is nonseismogenic as a consequence of the stable sliding behaviour of mixed layer clays that dehydrate at 100-150°C and perhaps from high pore pressures, (2) the seismogenic "locked" zone extending to about 350°C which allows elastic strain to accumulate, (3) the transition zone with stable sliding behaviour but with some coseismic displacement, that extends to about 450°C, and (4) the deep plastic zone.

The temperatures on the megathrust plane as a function of landward distance are found to be primarily dependent on (1) age of incoming oceanic plate, (2) thickness of sediment on incoming plate, (3) convergence rate, and (4) subducting plate dip angle. While a two-dimensional model has been applied, the temperatures on the thrust plane are found to be little different from simple one-dimensional steady state models where there is good surface heat flow data control. Thus, if the model results match the surface heat flow, the thermal conductivity in the accretionary prism is thus the most important uncertainty. The megathrust plane beneath the Cascadia margin is exceptionally hot as a consequence of the very young plate age and thick sediment section in Cascadia Basin. The 350° isotherm that is taken to mark the limit of stick-slip behaviour restricts the "locked" seismogenic zone to beneath the continental slope and outer shelf off southern Vancouver Island (Figure 12). The transition zone extends a similar distance further landward to the inner shelf. The seismogenic zone from the model results is found to be wider off Oregon compared to off southern Vancouver Island because of the slightly older subducting plate. It is much wider off the Olympic Peninsula because the plate is older and especially because the thrust dip angle is much shallower. More typical subduction zones such as central Chile are found to have thermally defined seismogenic zones that are much wider, commonly extending well beneath the coast.

The downdip extent of the transition zone from the thermal modelling is found to be comparable to the locked zone assuming the limits of 350 and 450°C. This agrees with the estimates from deformation data in Chile and Japan that there must be a transition zone approximately 100 km wide [*Savage*, 1989].

Even with detailed site specific modelling constrained by good structural and thermal data, there is at least a ±50°C uncertainty in the landward limit of the stick-slip to stable sliding transition (i.e., ±25°C in the temperature for the transition and ±25°C in the thermal modelling). This translates to about ±30 km in landward position for the Cascadia margin. An important

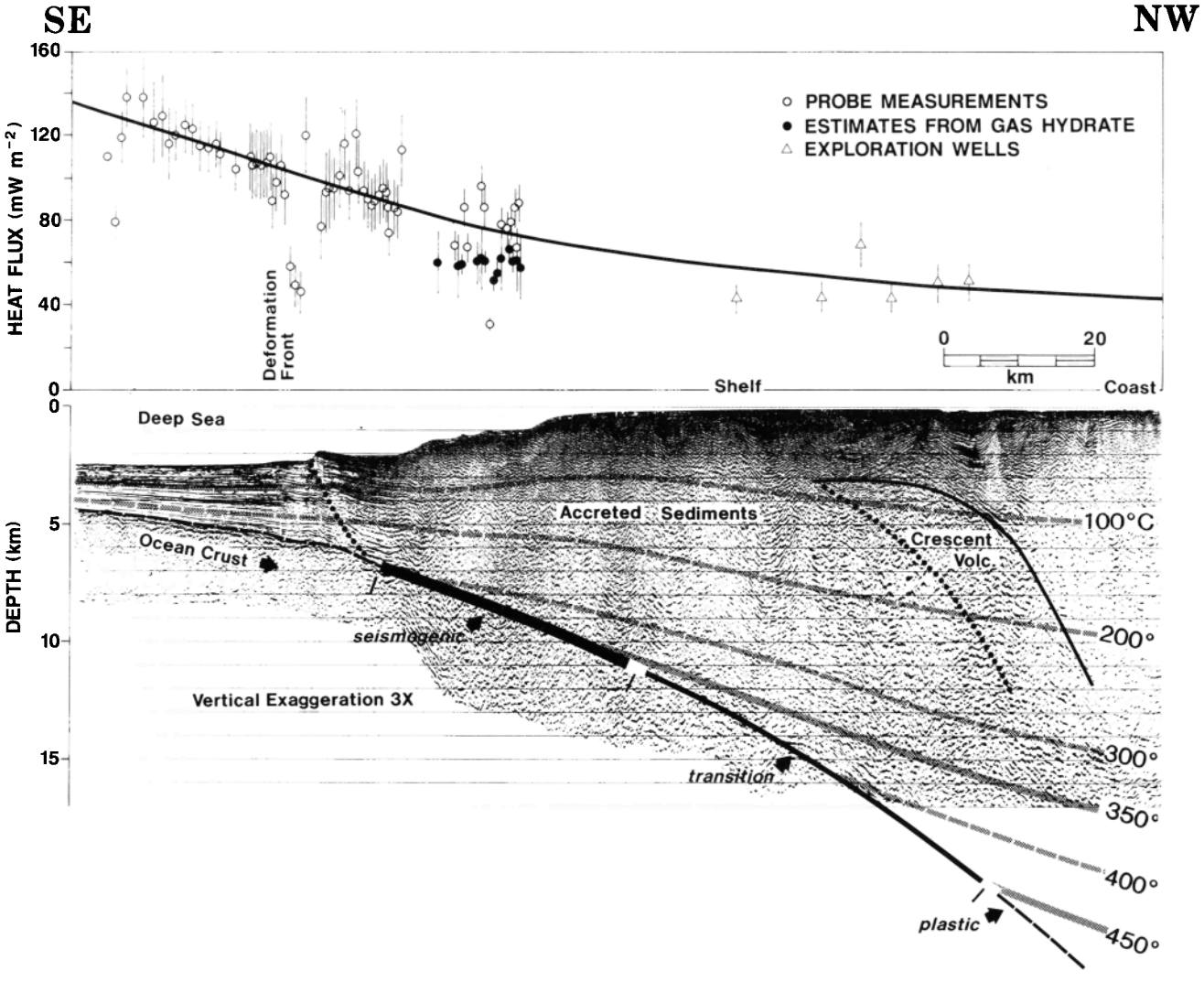

Fig. 12. Temperature cross-section from the marine portion of the preferred model superimposed on a seismic section across the southern Vancouver Island margin. The marine data and model heat flow are also shown.

uncertainty in modelled temperatures and thus the estimated position of the seismogenic zone in many subduction zones with thick sediment sections on the incoming oceanic plate, is the level of the detachment within the accretionary wedge. Another uncertainty in the width of the stick-slip zone that warrants further study is its seaward limit. Both stable sliding clays with high dehydration temperatures or high pore pressure could move this boundary landward and result in a much narrower seismogenic zone.

Support for the general position of the thermally controlled locked zone is provided by comparison of the horizontal and vertical interseismic deformation predicted by simple elastic dislocation models with the observed rates on the adjacent coastal regions. While the uncertainties in both the models and in the survey data are large, the main features appear to restrict the locked zone to be located offshore: (1) the observed crustal shortening in the coastal region accounts for only 10-20% of the plate convergence rate; (2) the observed vertical motion in the coastal region is everywhere up at a few millimetres per year. Interseismic upward motion agrees with the coseismic displacement being down along the coast as inferred from paleoseismic data [e.g., *Atwater,* 1987]. The locked zone being offshore resolves the apparent disagreement noted by *Ando and Balazs* [1979] between levelling data and the interseismic vertical motion expected from seismic subduction. Their deformation models assumed that the locked zone extended beneath the coast as commonly occurs beneath other subduction margins such as southern Japan. Such models have the hinge line landward of the coast, while our results indicate that it must be seaward.

The large variability in widths of the seismogenic zones inferred from thermal modelling for subduction zones around the world, may explain part of the large variation in the fraction of convergence estimated to be seismic [*Kanamori,* 1977]. Small seismic moment release rates may be a consequence of a narrow seismogenic zone, rather than a large part of the convergence being accommodated by aseismic slip.

The conclusion of a narrow offshore seismogenic zone should significantly affect the estimated ground motion and seismic hazard from subduction earthquakes in western British Columbia, Washington and Oregon. For example, the ground motion calculations for northwestern Washington suggested by *Cohee et al.* [1991] were based on an assumed location of the seismic zone based on comparison with other subduction zones such as Chile. Such a seismogenic thrust plane extends over 100 km further

landward than estimated by our model for the Olympic profile. The narrow seismogenic zone predicted by the thermal modelling restricts the maximum magnitude of thrust earthquakes on the margin, but if failure occurs simultaneously along most of the Cascadia margin in a manner comparable to the 1960 Chile event, very large earthquakes are still possible.

Complementary future work beyond the scope of this study is detailed comparison of the depths of the stick-slip and transition zones predicted by detailed site-specific thermal models with (1) the maximum downdip extent of seismic moment release in subduction zones on which major events have occurred, and (2) the pattern of coseismic and interseismic ground uplift and subsidence, for margins that have had major thrust events.

APPENDIX

Hutchison [1985] developed a theory of one-dimensional heat transfer in a sediment section during compaction. The crucial simplifying assumption is that the porosity of the sediment section always has the same decreasing function of depth only; i.e., at any time, for whatever sedimentation rate and sediment thickness, the porosity-depth profile is always the same. We use an exponential porosity function;

$$\phi = \phi_o \exp(-z/L) \qquad (A1)$$

where constants ϕ_o and L are derived by fitting (*A1*) to experimental values of porosity determined from seismic velocity data [e.g., *Davis et al.*, 1990]. A slight modification to (*A1*) occurs at a depth below which porosity is taken to remain at a nearly constant value, about $\phi_{min} = 0.15$. By further neglecting the compressibility of sediment matrix material and of the pore water, the constant porosity-depth profile uniquely determines the rates of upward pore water flow and sediment compaction deformation at any given time.

From the conservation of mass, for any pair of depths z_1 and z_2,

$$v_s(z_1,t)[1-\phi(z_1)] = v_s(z_2,t)[1-\phi(z_2)] \qquad (A2)$$

$$v_w(z_1,t)\,\phi(z_1) = v_w(z_2,t)\,\phi(z_2) \qquad (A3)$$

where v is velocity, and subscripts s and w denote sediment and water, respectively. Sediment and water velocities are readily determined from the boundary conditions, and the depth of the sediment-basement interface B is determined by solving $dB/dT = v_b$.

Once the velocities are determined, the thermal model of sedimentation and compaction is simply the solution of the heat conduction-convection equation;

$$\overline{\rho c}\,\frac{\partial}{\partial t} = \frac{\partial}{\partial z}\,\overline{\lambda}\frac{\partial T}{\partial z} - \overline{\rho c v}\,\frac{\partial T}{\partial t} + Q \qquad (A4)$$

where ρc is specific thermal capacity, λ is thermal conductivity, and Q is heat generation; a bar at the top denotes the average property of the matrix and pore fluid mixture. For basement, single constant values are used. For sediment;

$$\overline{\lambda} = \lambda_w^{\phi}\,\lambda_s^{(1-\phi)} \qquad (A5)$$

$$\overline{\rho c} = \rho c_w \phi + \rho c_s (1-\phi) \qquad (A6)$$

$$\overline{\rho c v} = \rho c_w v_w \phi + \rho c_s v_s (1-\phi) = v_b \overline{\rho c}(B) \qquad (A7)$$

The second equality in (*A7*) is a direct result of equations (*A2*) and (*A3*). The physical property values are listed in Table A1.

Based on seismic study and drill data, the sedimentation history on the seafloor of the Juan de Fuca plate experienced three phases. From the time of formation at about 6 Ma to 4 Ma there probably was very slow deposition because of the elevation of the spreading Juan de Fuca ridge. From 4 Ma to 2 Ma there was rapid primarily hemipelagic deposition and from about 2 Ma to the present there has been very rapid deposition of strongly layered turbidites. *Davis and Hyndman* [1989] have estimated the deposition rates for the latter two phases to be 1.1 mm yr^{-1} and 1.2 mm yr^{-1}, respectively. While the timing of these latter two phases is uncertain, the computed temperatures are insensitive to the exact intervals.

TABLE A1. List of Parameter Constants For A Cooling Juan de Fuca Plate With Sedimentation.

Parameter	Symbol	Value	Unit
Water conductivity	λ_w	0.6	W $m^{-1}K^{-1}$
Sediment conductivity	λ_s	2.74	W m^{-1} K^{-1}
Basement conductivity	λ_b	2.9	W m^{-1} K^{-1}
Water thermal capacity	ρc_w	4.30	MJ m^{-3} K^{-1}
Sediment thermal capacity	ρc_s	2.65	MJ m^{-3} K^{-1}
Basement thermal capacity	ρc_b	3.30	MJ m^{-3} K^{-1}
Sediment heat generation	Q	0.6	μW m^{-3}
Surface porosity	ϕ_o	0.6	
Porosity depth scale	L	1.5	km
Minimum porosity	ϕ_{min}	0.15	

The upper surface (water-sediment interface) is kept at 0°C, approximately that of the deep-sea floor. The lower boundary is chosen adequately deep (200 km) to approximate infinity and is maintained a temperature of 1400°C. The initial temperature is set at 1400°C. This simple model is based on the theory of a cooling half space used to explain the correlations between plate age, seafloor heat flux and topography. The success of the simple theory has been demonstrated by many authors (see review by *Davis*, [1989]).

Equation *(A4)* subject to the above boundary and initial conditions, and with the known sedimentation history, is solved with a one-dimensional, two-node finite element model. Within each element, temperature varies linearly, and the material properties and sediment and water velocities are taken as constants evaluated at the mid-point of the element. Smaller elements (typically 20 m) are used near the sediment surface where material properties and temperature vary the fastest, and very large elements can be used at depth. A deforming grid [*Wang and Davis*, 1991] is used to model accurately the moving boundary between sediment and basement. Time stepping is performed with a standard general finite difference scheme [e.g., *Huyakorn and Pinder*, 1983, p.56].

Having obtained the present temperature in the sediment column and the underlying basement as a function of depth, the lower boundary of the lithosphere is defined at the temperature of 1250°C. The temperatures for a 6 m.y. and a 8 m.y. old plate (i.e., near the deformation fronts off Vancouver Island and off the Olympic Peninsula and Oregon respectively, are shown in Figure A1 (also Figure 5a for sediment column temperatures).

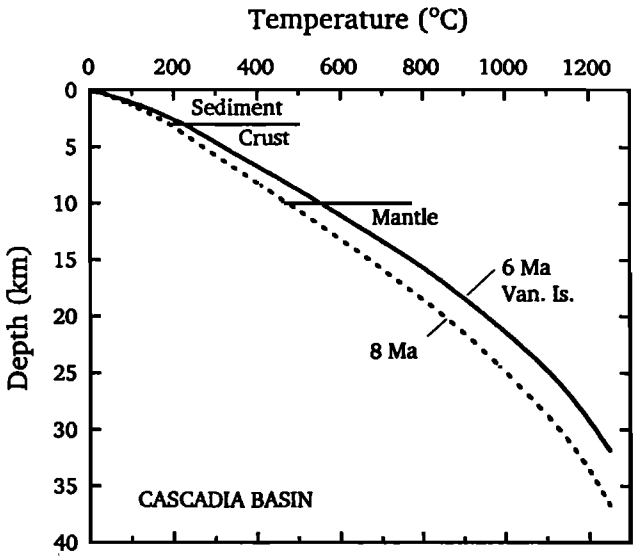

Fig. A1. Temperature-depth profiles computed for the sediment and basement just seaward of the deformation front off southern Vancouver Island (6 m.y. old oceanic plate), and off the Olympic Peninsula and northern Oregon (both 8 m.y. old plate). The zero depth is the sediment surface.

Acknowledgments. We wish to acknowledge very helpful discussions and unpublished data made available by G.C. Rogers, H. Dragert, M. Lisowski and J. Savage. Drafting and cartography were expertly provided by B. Sawyer and the P.G.C. drafting and photography team. Partial financial support to K. Wang was provided through the U.S. Geological Survey Extramural program. Geological Survey of Canada contribution 38191.

REFERENCES

Adams, J., Active deformation of the Pacific Northwest continental margin, *Tectonics, 3*, 449-472, 1984.

Adams, J., Paleoseismicity of the Cascadia subduction zone: Evidence from turbidites off the Oregon-Washington margin, *Tectonics, 9*, 569-583, 1990.

Anderson, R.N., S. Uyeda and A. Miyashiro, Geophysical and geochemical constraints at converging plate boundaries--Part I: Dehydration in the downgoing slab, *Geophys. J.R. Astron. Soc., 44*, 333-357, 1978.

Anderson, R.N., S.E., DeLong, and W.M., Schwarz, Thermal model for subduction with dehydration in the downgoing slab, *J. Geol., 86*, 731-739, 1976.

Ando, M., and E.I. Balazs, Geodetic evidence for aseismic subduction of the Juan de Fuca plate, *J. Geophys. Res., 84*, 3023-3028, 1979.

Atwater, B.F., Evidence for great Holocene earthquakes along the outer coast of Washington State, *Science, 236*, 942-944, 1987.

Atwater, B.F., Stuiver, M. and D.K. Yamaguchi, Radiocarbon test of earthquake magnitude at the Cascadia subduction zone, *Nature, 353*, 156-158, 1991.

Barr, T.D., and F.A. Dahlen, Thermodynamic efficiency and brittle frictional mountain building, *Science, 242*, 749-752, 1990.

Bathe, K.J., and E.L. Wilson, *Numerical Methods in Finite Element Analysis*, Prentice-Hall, Englewood Cliffs, N.J., 1976.

Blackwell, D.D., Heatflow analysis of the Cascadia subduction zone (How wide is the locked zone?), paper presented at Workshop on Oregon earthquake source zones, Oreg. State Univ., Corvallis, March 18, 1991.

Blackwell, D.D., J.L. Steele, and S. Kelley, Heat flow in the State of Washington and thermal conditions in the Cascade range, *J. Geophys. Res., 95*, 19,495-19,516, 1990.

Blanpied, M.L., D.A. Lockner, and J.D. Byerlee, fault stability inferred from granite sliding experiments at hydrothermal conditions, *Geophys. Res. Lett., 18*, 609-612, 1991.

Brace, W.F., and J.D. Byerlee, California earthquakes: Why only shallow focus?, *Science, 168*, 1573-1575, 1970.

Byerlee, J.D., Friction of rocks, *Pure Appl. Geophys., 116*, 615-626, 1978.

Byrne, D.E., D.M. Davis, and L.R. Sykes, Loci and maximum size of thrust earthquakes and the mechanics of the shallow region of subduction zones, *Tectonics, 7*, 833-857, 1988.

Byrne, T., and D. Fisher, Evidence for a weak and overpressured decollement beneath sediment-dominated accretionary prisms, *J. Geophys. Res., 95*, 9081-9097, 1990.

Calvert, A.J., and R.M. Clowes, Seismic evidence for the migration of fluids within the accretionary complex of western Canada, *Can. J. Earth Sci., 28*, 542-556, 1991.

Cande, S.C., and R.B. Leslie, Late Cenozoic tectonics of the southern Chile trench, *J. Geophys. Res., 91*, 471-496, 1986.

Cande, S.C., R.B. Leslie, J.C. Parra and M. Hobart, Interaction between the Chile ridge and Chile trench: Geophysical and geothermal evidence, *J. Geophys. Res., 92*, 495-520, 1987.

Carson, B., Tectonically induced deformation of deep-sea sediments off Washington and northern Oregon: Mechanical consolidation, *Marine Geol., 24*, 289-307, 1977.

Chamley, H., *Clay Sedimentology*, 243 p, Springer-Verlag, New York, 1989.

Chen, W., and P. Molnar, Focal depths of intracontinental and interplate earthquakes and its implications for the thermal and mechanical properties of the lithosphere, *J. Geophys. Res., 88*, 4183-4214, 1983.

Clague, J., J.R. Harper, R.J. Hebda, and D.E. Howes, Late Quaternary sea levels and crustal movements, coastal British Columbia, *Can. J. Earth Sci., 19*, 597-618, 1982.

Cochrane, G.R., B.T.R. Lewis, and K.J. McClain, Structure and subduction processes along the Oregon-Washington margin, *Pure and Appl. Geophys., 128*, 767-800, 1988.

Cohee, B.P., P.G. Somerville, and N.A. Abrahamson, Simulated ground motions for hypothesized M_w=8 subduction earthquakes in Washington and Oregon, *Bull. Seismol. Soc. Am., 81*, 28-56, 1991.

Crosson, R.S., and T.J. Owens, Slab geometry of the Cascadia subduction zone beneath Washington from earthquake hypocenters and teleseismic converted waves, *Geophys. Res. Lett., 14*, 824-827, 1987.

Darienzo, M.E., and C.D. Peterson, Episodic tectonic subsidence of Late Holocene salt marshes, northern Oregon, central Cascadia margin, *Tectonics, 9*, 1-22, 1990.

Davis, E.E., Thermal aging of oceanic lithosphere, in *CRC Handbook of Seafloor Heatflow*, edited by J.A. Wright and K.E. Louden, pp. 145-167, CRC Press, Boca Raton, Fl., 1989.

Davis, E.E., and R.D. Hyndman, Accretion and recent deformation of sediments along the northern Cascadia subduction zone, *Geol. Soc. Am., 101*, 1465-1480, 1989.

Davis, E.E., and J.L. Karsten, On the asymmetric distribution of seamounts about the Juan de Fuca Ridge: Ridgecrest migration over a heterogeneous asthenosphere, *Earth Planet. Sci. Lett., 79*, 385-396, 1986.

Davis, E.E., R.D. Hyndman, and H. Villinger, Rates of fluid expulsion across the northern Cascadia accretionary prism: Constraints from new heat flow and multichannel seismic reflection data, *J. Geophys. Res., 95*, 8869-8889, 1990.

DeMets, C., R.G. Gordon, S. Stein, and D.F. Argus, A revised estimate of Pacific-North America motion and implications for western North America plate boundary zone tectonics, *Geophys. Res. Lett., 14*, 911-914, 1987.

Dieterich, J., Constitutive properties of faults with simulated gouge, in *Mechanical Behaviour of Crustal Rocks, Geophys. Monogr. Ser.*, Vol. 24, edited by N.L. Carter et al., pp.103-120, A.G.U., Washington, D.C., 1981.

Douglas, B.C., Global sea level rise, *J. Geophys. Res., 96*, 6981-6992, 1991.

Drew, J.J., and R.M. Clowes, A re-interpretation of the seismic structure across the active subduction zone of western Canada, in Studies of Laterally Heterogeneous Structures Using Seismic Refraction and Reflection Data, edited by A.G. Green, *Geol. Surv. Can. Pap., 890-13,* 115-132, 1990.

Dumitru, T.A., Effects of subduction parameters on geothermal gradients in forearcs, with an application to Franciscan subduction in California, *J. Geophys. Res., 96,* 621-641, 1991.

Engebretson, D.C., A. Cox and G.A. Thompson, Relative motions between oceanic and continental plates in the Pacific Basin, *Spec. Pap. Geol. Soc. Am., 206,* 59 p; 1985.

Ghomshi, M.M., J. Arkani-Hamed, D.W. Strangway, and R.D. Russell, Underplating of oceanic lithosphere in the Archean: a possible mechanism for the formation of Archean komatiites, *Tectonophysics, 172,* 291-302, 1990.

Green, A.G. (Ed.), Studies of laterally heterogeneous structures using seismic refraction and reflection data, *Geol. Surv. Can. Pap., 890-13,* 224 p, 1990.

Gu, J.C., J.R. Rice, A.L. Ruina, and S.T. Tse, Slip motion and stability of a single degree of freedom elastic system with rate and state dependent friction, *J. Mech. Phys. Solids, 32,* 167-196, 1984.

Hasebe, K., N. Fujii, and S. Uyeda, Thermal processes under island arcs, *Tectonophysics, 10,* 335-355, 1970.

Heaton, T.H., The calm before the quake?, *Nature, 343,* 511-512, 1990.

Heaton, T.H., and S.H. Hartzell, Earthquake hazards on the Cascadia subduction zone, *Science, 236,* 162-168, 1987.

Heaton, T.H. and H. Kanamori, Seismic potential associated with subduction in the northwestern United States, *Bull. Seismol. Soc. Am., 74,* 933-944, 1984.

Hicks, S.D., An average geopotential sea level series for the United States, *J. Geophys. Res., 83,* 1377-1379, 1978.

Holdahl, S.R., F. Faucher and H. Dragert, Contemporary vertical crustal motion in the Pacific Northwest, in *Slow Deformation and Transmission of Stress in the Earth, Geophys. Monogr. Ser.,* vol. 49, edited by S.C Cohen and P. Vanicek, pp. 17-29, A.G.U., Washington, D.C., 1989.

Hower, J., W.V. Eslinger, M. Hower, and E.A. Perry, Mechanism of burial metamorphism of argillaceous sediments, I. Mineralogical and chemical evidence, *Geol. Soc. Am. Bull., 87,* 725-737, 1976.

Hutchison, I., The effects of sedimentation and compaction on oceanic heat flow, *Geophys. J.R. Astron. Soc., 82,* 439-459, 1985.

Huyakorn, P.S., and G.F. Pinder, *Computational Methods in Subsurface Flow,* Academic, San Diego, Calif., 1983.

Hyndman, R.D., and D.H. Weichert, Seismicity and rates of relative motion on the plate boundaries of western North America, *Geophys. J. R. Astron. Soc., 72,* 59-82, 1983.

Hyndman, R.D., G.C. Rogers, and H. Dragert, Thermal, pore pressure and vertical deformation limits on the zone of major thrust earthquake failure beneath the Vancouver Island subduction zone (abstract), *Seismol. Res. Lett., 60,* 2, 1989.

Hyndman, R.D., C.J. Yorath, R.M. Clowes, and E.E. Davis, The northern Cascadia subduction zone at Vancouver Island: Seismic structure and tectonic history, *Can. J. Earth Sci. 27,* 313-329, 1990.

Hyndman, R.D., and E.E. Davis, A mechanism for the formation of methane hydrate and seafloor bottom-simulating reflectors by vertical fluid expulsion, *J. Geophys. Res., 97,* 7025-7041, 1992.

Jennings, S., and G.R. Thompson, Diagenesis of Plio-Pleistocene sediments of the Colorado River delta, southern California, *J. Sediment Petrol., 56,* 89-98, 1986.

Kanamori, H., Seismic and aseismic slip along subduction zones and their tectonic implications, in *Island Arcs, Deep-sea Trenches and Back-Arc Basins, Maurice Ewing Ser.,* vol. 1, edited by M. Talwani and W.C. Pitman, pp.163-174, A.G.U., Washington, D.C., 1977.

Kanamori, H., Rupture process of subduction-zone earthquakes, *Annu. Rev. Earth Planet. Sci., 14,* 293-322, 1986.

Koch, P.S., J.M. Christie, and R.P. George, Flow law of "wet" quartzite in the α-quartz field, *EOS, Trans. A.G.U., 61,* 376, 1980.

Kulm, L.D., et al., *Initial Reports of the Deep Sea Drilling Project,* vol. 18, U.S. Government Printing Office, Washington, D.C., 1973.

Lachenbruch, A. and J.H. Sass, Heat flow and energetics of the San Andreas fault zone, *J. Geophys. Res., 85,* 6185-6222, 1980.

Lachenbruch, A., and J.H. Sass, Heat flow from Cajon Pass, fault strength, and tectonic implications, *J. Geophys. Res., 97,* 4995-5015, 1992.

LePichon, X., P. Henry, and S. Lallemant, Water flow in the Barbados Accretionary Complex, *J. Geophys. Res., 95,* 8945-8967, 1990.

Lewis, T.J., Heat flux in the Canadian Cordillera, in *Neotectonics of North America,* Map Volume, edited by D.B. Slemmons, E.R. Engdahl, D.D. Blackwell, and D. Schwartz, Decade of North American Geology Series, Geological Society of America, Boulder, Colo. 1990.

Lewis, T.J. and W.H. Bentkowski, Potassium, uranium and thorium concentrations of crustal rocks: a data file, *Geol. Surv. Can. Open File Rep., 1744,* 1988.

Lewis, T.J., W.H. Bentkowski, E.E. Davis, R.D. Hyndman, J.G. Souther, and J.A. Wright, Subduction of the Juan de Fuca plate: thermal consequences, *J. Geophys. Res., 93,* 15,207-15,225, 1988.

Lewis, T.J., W.H. Bentkowski, and J.A. Wright, Thermal state of the Queen Charlotte Basin, British Columbia: warm, in Evolution and Hydrocarbon Potential of the Queen Charlotte Basin, British Columbia, Geol. Surv. Can. Pap., 90-10, 489-506, 1991.

Lewis, T.J., W.H. Bentkowski and R.D. Hyndman, Crustal temperatures near the LITHOPROBE southern Canadian Cordilleran transect, *Can. J. Earth Sci., 29,* 1197-1214, 1992.

Lisowski, M., W.H. Prescott, H. Dragert, and S.R. Holdahl, Results from 1986 and 1987 GPS survey across the Strait of Juan de Fuca, Washington and British Columbia (abstract), *Seismol. Res. Lett., 60,* 1, 1989.

Logan, J., and J. Rauenzahn, Frictional dependence of gouge mixtures of quartz and montmorillonite on velocity, composition and fabric, *Tectonophysics, 144,* 87-108, 1987.

MacKay, M.E., G.F. Moore, G.R. Cochrane, J.C. Moore, and L.D Kulm, Landward vergence and oblique structural trends in the Oregon margin accretionary prism: implications and effect on fluid flow, *Earth Planet. Sci. Lett., 109,* 477-491, 1992.

McKenzie, D.P., Temperature and potential temperature beneath island arcs, *Tectonophysics, 10,* 357-366, 1970.

Melosh, H.J., and A. Raefsky, Anelastic response of the earth to a dip-slip earthquake, *J. Geophys. Res., 88,* 515-526, 1983.

Minear, J.W., and M.N. Toksoz, Thermal regime of a downgoing slab and new global tectonics, *J. Geophys. Res., 75,* 1397-1419, 1970.

Molnar, P., and P. England, Temperatures, heat flux, and frictional stress near major thrust faults, *J. Geophys. Res., 95,* 4833-4856, 1990.

Moore, G.F., T.H. Shipley, P.L. Stoffa, D.E. Karig, A. Taira, S. Kuramoto, H. Tokuyama, and K. Suyehiro, Structure of the Nankai Trough accretionary zone from multichannel seismic reflection data, *J. Geophys. Res., 95,* 8,753-8,765, 1990.

Moore, J.C., and P. Vrolijk, Fluids in accretionary prisms, *Rev. Geophys., 30,* 113-135, 1992.

Peltier, W.R., and A.M. Tushingham, Global sea level rise and the greenhouse effect: Might they be connected? *Science, 244,* 806-810, 1989.

Plafker, G., and J.C. Savage, Mechanism of the Chilean earthquake of May 21, 1960, *Geol. Soc. Am. Bull., 81,* 1001-1030, 1970.

Rice, J.R., and A.L. Ruina, Stability of steady frictional slipping, *J. Appl. Mech., 105,* 343-349, 1983.

Riddihough, R.P., Contemporary movements and tectonics on Canada's west coast: A discussion, *Tectonophys., 86,* 319-341, 1982.

Riddihough, R.P., Recent movements of the Juan de Fuca plate system, *J. Geophys. Res., 89,* 6980-6994, 1984.

Riddihough, R.P. and R.D. Hyndman, Canada's active western margin-The case for subduction, *Geosci. Can., 3,* 269-278, 1976.

Rogers, G.C., Some comments on the seismicity of the northern Puget Sound-southern Vancouver Island region, in Earthquake Hazards of the Puget Sound Region, Washington, edited by J.C. Yount and R.S. Crosson, *U.S. Geol. Surv. Open File Rep. 83-19,* 19-27, 1983.

Rogers, G.C., Seismicity beneath the LITHOPROBE corridor, paper presented at symposium on the Deep Structure of Southern Vancouver

Island: Results of LITHOPROBE Phase 1, Geol. Assoc. Can., Pacific Section, Victoria, B.C., 1985.

Rogers, G.C., An assessment of the megathrust earthquake potential of the Cascadia subduction zone, *Can. J. Earth Sci., 25*, 844-852, 1988.

Rogers, G.C., C. Spindler, and R.D. Hyndman, Seismicity along the Vancouver Island LITHOPROBE corridor, paper presented at LITHOPROBE Southern Cordillera symposium, Univ. of Calgary, Alberta, 1990.

Ruff, L.J., Do trench sediments affect great earthquake occurrence in subduction zones? *Pure and Appl. Geophys., 1/2*, 263-282, 1989.

Ruff, L.J., and H. Kanamori, Seismic coupling and uncoupling at subduction zones, *Tectonophysics, 99*, 99-117, 1983.

Ruina, A.L., Slip instability and state variable friction laws, *J. Geophys. Res., 88*, 10,359-10,370, 1983.

Savage, J.C., A dislocation model of strain accumulation and release at a subduction zone, *J. Geophys. Res., 88*, 4984-4996, 1983.

Savage, J.C., Aseismic slip in seismic gaps at subduction zones (abstract), *Seismol. Res. Lett., 60*, 2, 1989.

Savage, J.C., M. Lisowski, and W.H. Prescott, Strain accumulation in western Washington, *J. Geophys. Res., 96*, 14,493-14,507, 1991.

Scholtz, C.H., Mechanics of faulting, *Annu. Rev. Earth Planet. Sci., 17*, 309-334, 1988.

Scholtz, C.H., *The Mechanics of Earthquakes and Faulting*, 439 pp., Cambridge University Press, New York, 1990.

Shi, Y., C. Wang, M.G. Langseth, M. Hobart and R. von Huene, Heat flow and thermal structure of the Washington-Oregon accretionary prism-A study of the lower slope, *Geophys. Res. Lett., 15*, 1113-1116, 1988.

Shouldice, D.H., Geology of the western Canadian continental shelf, *Can. Soc. Petrol. Geol. Bull., 19*, 405-424, 1971.

Silver, E.A., Pleistocene tectonic accretion of the continental slope off Washington, *Marine Geol., 13*, 239-249, 1972.

Snavely, P.D., and H.C. Wagner, Geologic cross section across the continental margin off Cape Flattery, Washington, *U.S. Geol. Surv. Open File Rep., 81-0978*, 1981.

Snavely, P.D., Tertiary geologic framework, neotectonics, and petroleum potential of the Oregon-Washington continental margin, in *Geology and Resource Potential of the Continental Margins of Western North America and Adjacent Basins–Beaufort Sea to Baja California*, edited by D.W. Scholl, A. Grantz, and J. Vedder, pp. 305-335, U.S. Geological Survey, Menlo Park, Calif. 1987.

Snay, R.A., and T. Matsikari, Horizontal deformation in the Cascadia subduction zone as derived from serendipitous geodetic data, *Tectonophysics, 194*, 59-67, 1991.

Spence, W., Stress origin and earthquake potentials in Cascadia, *J. Geophys. Res., 94*, 3,076-3,088, 1989.

Spence, G.D., R.M. Clowes, and R.M. Ellis, Seismic structure across the active subduction zone of western Canada, *J. Geophys. Res., 90*, 6754-6772, 1985.

Spence, G.D., R.D. Hyndman, S.G. Langton, E.E. Davis, and C.J. Yorath, Multichannel seismic reflection profiles across the Vancouver Island continental shelf and slope, *Geol. Surv. Can., Open File Rep. 2391*, 1991a.

Spence, G.D., R.D. Hyndman, E.E. Davis, and C.J. Yorath, Seismic structure of the northern Cascadia accretionary prism: Evidence from new multichannel seismic reflection data, in *Continental Lithosphere: Deep Reflections*, Geodynamics 22, A.G.U., Washington, D.C., 257-263, 1991b.

Stesky, R., The mechanical behaviour of faulted rock at high temperature and pressure, Ph.D. thesis, Mass. Inst. of Technol., Cambridge, 1975.

Stock, J.M., and P. Molnar, Uncertainties and implications of the Late Cretaceous and Tertiary positions of North America relative to the Farallon, Kula and Pacific plates, *Tectonics, 7*, 1339-1384, 1988.

Stuart, W.D., Forecast model for great earthquakes at the Nankai Trough subduction zone, *Pure Appl. Geophys., 126*, 619-641, 1988.

Sydora, L.J., F.W. Jones and R. St.J. Lambert, The thermal regime of the descending lithosphere: The effect of varying the angle and rate of subduction, *Can. J. Earth. Sci., 15*, 626-641, 1978.

Taber, J.J., and B.T.R. Lewis, Crustal structure of the Washington continental margin from refraction data, *Bull. Seismol. Soc. Am., 76*, 1011-1024,1986.

Tabor, R.W., and W.M. Cady, The structure of the Olympic Mountains, Washington-Analysis of a subduction zone, *U.S. Geol. Surv. Prof. Pap., 1033*, 1978.

Thatcher, W., and J.B. Rundle, A viscoelastic coupling model for the cyclic deformation due to periodically repeated earthquakes at subduction zones, *J. Geophys. Res., 89*, 7631-7640, 1984.

Tichelaar, B.W., and L.J. Ruff, Seismic coupling along the Chilean subduction zone, *J. Geophys. Res., 96*, 11,997-12,022, 1991.

Tichelaar, B.W., and L.J. Ruff, Depth of seismic coupling along subduction zones, *J. Geophys. Res.*, in press, 1992.

Tse, S.T., and J.R. Rice, Crustal earthquake instability in relation to the depth variation of frictional slip properties, *J. Geophys. Res., 91*, 9,452-9,472, 1986.

Turcotte, D.L., and G. Schubert, *Geodynamics: Applications of Continuum Physics to Geological Problems*, John Wiley, New York, 1982.

Tushingham, A.M. and W.R. Peltier, Ice-3G: A new global model of late Pleistocene de-glaciation based upon geophysical predictions of post-glacial relative sea level change, *J. Geophys. Res., 96*, 4497-4523, 1991.

van de Beukel, J., and R. Wortel, Temperatures and shear stresses in the upper part of a subduction zone, *Geophys. Res. Lett., 14*, 1057-1060, 1987.

van de Beukel, J., and R. Wortel, Thermo-mechanical modelling of arc-trench regions, *Tectonophysics, 154*, 177-193, 1988.

Velde, B., *Clay Minerals. A Physical-Chemical Explanation of their Occurrence*, 218 pp., Elsevier, New York, 1985.

von Huene, R., and D.W. Scholl, Observations at convergent margins concerning sediment subduction, subduction erosion, and growth of continental crust, *Rev. Geophys., 29*, 279-316. 1991.

Vrolijk, P., On the mechanical role of smectite in subduction zones, *Geology, 18*, 703-707, 1990.

Wang, C.Y., Sediment subduction and frictional sliding in a subduction zone, *Geology, 8*, 530-533, 1980.

Wang, C.Y., and N.H. Mao, Shearing of rock joints with saturated clays at high confining pressures, *Geophys. Res. Lett., 6*, 825-828, 1979.

Wang, C.Y., and Y.L. Shi, On the thermal structure of subduction complexes: a preliminary study, *J. Geophys. Res., 89*, 7,709-7,718, 1984.

Wang, K., An inverse finite element method for the study of steady state terrestrial heat flow problems, Ph.D. thesis, Univ. of West. Ont., London, 1989.

Wang, K., and E.E. Davis, Thermal effects of marine sedimentation in hydrothermally active areas, *Geophys. J. Int., 110*, 70-78, 1992.

Wiens, D.A., and S. Stein, Age dependence of oceanic intraplate seismicity and implications for lithospheric evolution, *J. Geophys. Res., 88*, 6455-6468, 1983.

Wigen, S.O., and F.E. Stephenson, Mean sea level on the Canadian West Coast, in *Proceedings of 2nd International Symposium on Problems Related to the Redefinition of North American Vertical Geodetic Networks (NAD)*, pp. 105-124, Canadian Institute of Surveying, Ottawa, Ont., 1980.

Wong, I.G., and D.S. Chapman, Deep intraplate earthquakes in the western United States and their relationship to lithospheric temperatures, *Bull. Seismol. Soc. Am., 80*, 589-599, 1990.

Ziagos, J.P., D.D. Blackwell, and F. Mooser, Heat flow in southern Mexico and the thermal effects of subduction, *J. Geophys. Res., 90*, 5410-5420, 1985.

R.D. Hyndman and K. Wang, Geological Survey of Canada, Pacific Geoscience Centre, P.O. Box 6000, Sidney, B.C., Canada V8L 4B2.

(Received December 2, 1991;
revised September 8, 1992;
accepted September 15, 1992.)